2.02

Stability of Elastic, Anelastic, and Disintegrating Structures, and Finite Strain Effects: an Overview

Z. P. BAŽANT

Northwestern University, Evanston, IL, USA

2.02.1 INTRODUCTION

Stability is a fundamental problem of solid mechanics whose solution determines the ultimate loads at which structures fail or deflect excessively. It is an old problem which has been studied for two and half centuries. The evolution of the theory was for a long time focused on elastic structures for which the loss of stability is the primary cause of failure, the material strength having little or no relevance. Throughout the twentieth century, interest gradually expanded to anelastic structures where stability loss and material failure are intertwined due to plastic behavior and creep. Since the mid-1970s, the destabilizing effects of material disintegration caused by damage

localization and fracture propagation, as well as the finite strain effects on stability of three-dimensional (3D) bodies, have received enormous attention. Thus, as of early 2000s, the theory of structural stability may be seen as a very broad field which encompasses most of solid mechanics and intersects with most if its domains, while resting on the same basic concepts and utilizing the same mathematical approaches.

The present chapter, taking this very broad viewpoint, will attempt a synthesizing review of the main results in the entire field of stability theory as it exists today. The rich spectrum of results in the classical theory of elastic stability, including the difficult but beautiful subject of shell bucking, can be covered only succinctly in this, admittedly overambitious, review. An enhanced emphasis, out of proportion to the scope of existing results, will be placed on anelastic structures, especially on the challenging modern problems of stability of structures losing their integrity because of distributed damage or localized fracture, and on the finite strain effects in 3D bodies, an intriguing topic that has been generating controversies and lively polemics for almost a century. The discussion will focus on these "hot" topics in much more detail than other stability studies. While the first two sections are of a review character, the last section, devoted to 3D finite strain effects on stability, will present in considerable detail a new explanation of the differences between the Engesser- and Haringx-type theories of sandwich buckling, widely regarded as paradoxical.

To avoid excessive length and to make this review easily accessible to engineers and scientists from other fields desiring to acquaint themselves with structural stability theory, mathematics will be kept to the bare minimum. The differential equations as well as the derivations will be omitted. Nevertheless, to enhance understanding, the physical causes and mechanisms of various types of instabilities will be discussed, albeit concisely.

Apart from some selected contributions, only the main literature sources to the vast field of stability can be cited here. Extensive literature references and a detailed exposition of most of the material covered here can be found in the book by Bažant and Cedolin (1991). Perspicacious reviews of the more classical material on elastic and plastic stability, considerably more detailed and much more mathematical, were given by Hutchinson (1974) and Budianski and Hutchinson (1972), and a valuable review of experimental evidence is found in Singer *et al.* (1998). The earlier works are covered in Timoshenko and Gere (1961).

2.02.2   ELASTIC STRUCTURES

2.02.2.1   Buckling of Columns, Frames, and Arches

The primary cause of failure of slender elastic beams or frames carrying large compressive axial forces due to gravity loads is not failure of the material but attainment of Euler's (1744) first critical load,

$$P_{\mathrm{cr}1} = \left(\frac{\pi^2}{L^2}\right) EI \qquad (1)$$

where E = Young's modulus, I = centroidal moment of inertia of the cross-section, and L = effective length representing the half-wavelength of deflection curve, which depends on the boundary conditions. For the idealized case of a perfect structure, P_{cr} represents a state of neutral equilibrium (i.e., a state at which the deflections can increase at constant load), and a state of symmetry-breaking bifurcation of the equilibrium path in the load-deflection space. The critical stress

$$\sigma_{\mathrm{cr}} = \frac{P_{\mathrm{cr}}}{A} = \frac{\pi^2 E}{(L/r)^2} \qquad (2)$$

where A = cross-section area and $r^2 = I/A$, depends only on E and the slenderness L/r, and exhibits no size effect.

The analysis of beam or column buckling requires that the deflections of the structure be taken into account in writing the differential equations of the beam or frame based on the theory of bending. For reasons of geometry, the problem is nonlinear at large deflections, but linearization for small deflections leads to a linear fourth-order ordinary differential equation for the deflections. The critical load is found from a linear eigenvalue problem.

Real columns inevitably have imperfections such as an initial curvature, axial load eccentricity, or small lateral loads, and often are subjected to large initial bending moments M^0. Because of the imperfections, the deflection increases rapidly when $P_{\mathrm{cr}1}$ is approached. Small deflections w near P_{cr} are given by Young's (1807) formula

$$w = \frac{w_0}{1 - (P/P_{\mathrm{cr}1})} \qquad (3)$$

where constant w_0 characterizes the initial imperfection or initial bending moments. While this formula is exact only for initial sinusoidal curvature, it represents an asymptotic approximation near $P_{\mathrm{cr}1}$ for all kinds of initial imperfections. Therefore it has been adopted as a universal basis of design codes (a less simple formula, which was used for steel

structures, is obtained for an eccentric load but it is asymptotically equivalent near the critical load). The deflection given by Young's formula is used to calculate the initial moment magnification by P and w. The magnification has a factor depending on the initial moment distribution along the column, which is given in design codes by approximate formulas.

Although the basic cases of critical loads of columns with various end conditions were solved by Euler as early as 1744 (long before the theory of bending was completed by Navier), developments in column theory have nevertheless proceeded until modern times. Simple but realistic design formulas taking into account geometrical imperfections and initial bending moments in metallic and concrete columns or frames were incorporated into design codes by the middle of the twentieth century.

The curve of finite deflections of very slender elastic columns of constant cross-section (a curve called the "*elastica*") was solved exactly (Kirchhoff, 1859) in terms of elliptic integrals. Very large deflections of arbitrary elastic columns and frames can today be easily calculated by nonlinear finite element (FE) codes.

Many extensions of the column buckling theory have been studied. The basic cases of spatial buckling of beams subjected to axial force and various kinds of torque are amenable to simple analytical solutions. If the column is not slender, or if it is orthotropic, with a low shear modulus (as in fiber composites), the bending theory must be enhanced by taking into account shear deformations, which can substantially decrease the value of critical load (note a later comment on the formal equivalence but different applicability of the Engesser and Haringx formulas). Consideration of the effect of pressure in compressed fluid-filled pipes, or of axial pre-stress introduced by embedded tendons, is a problem appearing at first tricky but in fact easy to handle.

The buckling of elastic frames, i.e., assemblages of rigidly or flexibly connected beams, is normally analyzed by the stiffness method, on the basis of the stiffness matrices of beam elements. The stiffness matrix relates the increments of the bending moments and shear and axial forces at the ends of the element to the increments of the associated displacements and rotations. Because of the second-order moments of the initial axial force on the deflections, the stiffness coefficients depend on the axial force. If the beam has a uniform cross section, this dependence can be described by simple trigonometric, hyperbolic and polynomial functions of the initial axial load,

derived by James (1935) and Livesley and Chandler (1956) and others. Trigonometric expressions for the inverse flexibility matrix coefficients were derived earlier by von Mises and Ratzensdorfer (1926) and Chwalla (1928).

There are two possible approaches to calculating the critical loads of frames: (i) the beam is subdivided into many sufficiently short beam elements, in which case the dependence of the stiffness matrix on the initial axial force gets automatically linearized and the critical load (or parameter of the load system) can then be obtained from a linear matrix eigenvalue problem; or (ii) the stiffness matrix of the entire beam is used. In the latter approach, the number of unknowns is one or two orders of magnitude less but the matrix eigenvalue problem is nonlinear because the stiffness coefficients are highly nonlinear functions of the load. The latter approach is computationally far more efficient but requires a more complicated iterative solution based on successive tangential linearizations of the stiffness matrix.

Designers sometimes simplify the frame buckling problem by considering a column within the frame as a separate elastic column with flexible end restraints, isolated from the frame. However, such a trivialization often involves large errors on the unsafe side because the dependence of the effective tangential stiffness of the end restraints on the unknown critical load is neglected.

The redundant internal forces in frames can vary at the critical state while the load is constant. This means that the flexibility matrix of the primary statically determinate structure becomes singular at the critical load. Typically, however, the coefficients of this matrix become infinite and the matrix loses positive definiteness before the critical load is reached. This makes the flexibility matrix unsuitable for checking stability and the flexibility method computationally unsuitable for structures with more than a few redundant internal forces.

Very large regular rectangular frames or lattices lead to linear difference equations. The basic cases can then be solved exactly by the methods of difference calculus (Bažant and Cedolin, 1991, Section 2.02.3). The simplest modes, easily solved by one-line formula, are the internal buckling of either sway or nonsway type, and the boundary buckling. Approximating the difference equations as partial differential equations (Bažant, 1971b), one can solve the long-wave (global) buckling of the frame as a continuum. Because the rotations ϕ of the joints are independent of the rotations θ of the chords of the beams, the proper approximation (Bažant, 1971b, Bažant and Cedolin, 1991,

section 2.10), which must be exact up to the second-order terms, is the micropolar continuum. (Be warned that several micropolar approximations found in the literature are incorrect because cross terms such as $\phi\phi_{,xx}$ are missing yet contribute to the quadratic terms of energy density ($x =$ spatial coordinate).) The critical loads of large regular frames or lattices with rectangular boundaries were thus solved in 1973 analytically (Bažant and Cedolin, 1991). Various types of built-up or latticed columns can be continuously approximated as a continuous column but the shear deformation must be taken into account (see later comments on the Engesser and Haringx formulas).

An intricate case for which a sophisticated special theory has evolved (cf. Bažant and Cedolin, 1991, section 2.8) is the buckling of high arches and slender rings (or cylindrical shells in the transverse plane). Their buckling is described by a fourth-order linear differential equation for arch deflections. Its coefficients are not constant but vary along the arch with its initial curvature. They also depend on the load in a more complicated way than in the case of columns. The axial inextensibility of the arch, which is a justifiable simplifying assumption for high (or deep) arches, presents further restrictions. In the case of hinged arches, the inextensibility constraint excludes the odd-numbered critical loads, which correspond to buckling modes with an odd number of waves. (Noting this restriction, Hurlbrink (1908) corrected the previously accepted Boussinesq solution of the lowest critical value of uniform load.)

2.02.2.2 Dynamic Stability Analysis and Chaos

Up to now, we tacitly implied the loads to be conservative. Such problems can be solved statically and do not necessitate the use of the general criterion of stability, which is dynamic. However, for structures subjected to nonconservative loads, stability may, and often is, lost in a dynamic manner. Important examples of nonconservative loads are: (i) loads with prescribed time variation (e.g., pulsating loads), (ii) loads generated by the flow of gases (wind loads) or liquids, and (iii) reactions from jet or rocket propulsion. An idealization of (ii) and (iii) are the follower loads, whose orientation follows the rotation of the structure.

The fundamental definition of stability that is generally accepted in all fields of science is due to Liapunov (1893) and may be simply stated as follows. A given solution (or, as a special case, a given equilibrium state) of a dynamic system is stable if all the possible *small* perturbations of the initial conditions can lead only to *small* changes of the solution (or response). (In the case of continuous structures, it makes sense to measure the changes in terms of an overall norm of the deflection distribution rather than locally.)

Based on Liapunov's definition, it can be shown that, under certain mild restrictions, stability can be decided by analyzing a linearized system. This, for instance, justifies considering only linearized small-strain expressions in columns, plates, and shells. Stable systems, when perturbed, develop vibrations, either undamped or damped. The vibration frequency depends on the applied load.

It is further easily proved that stability is lost when the frequency of natural vibrations becomes complex (Borchhardt's criterion). In conservative systems, the frequency diminishes with increasing static load and becomes zero at the limit of stability, which represents the critical state of neutral equilibrium (Figure 1(a)). Stability is then lost through nonaccelerated (static) motion away from the initial equilibrium state, called the divergence (for aircraft wings) or (more generally) static buckling.

An important property of nonconservative systems is that the frequency at the loss of stability can be nonzero (Figure 1(b)), in which case a static stability analysis is inapplicable. Typically, dynamic instability is caused by vibrations of ever increasing amplitude, during which the structure moves in such a manner that it absorbs an unbounded amount of energy from the nonconservative load (such as wind or pulsating load). The dynamic instability, also called flutter, is an important consideration for aircraft wings, as well as tall guyed masts, chimneys and suspension bridges (Simiu and Scanlan, 1986). A famous example is the aeroelastic instability that destroyed the Tacoma Narrows Bridge in 1940.

Pulsating loads, produced, e.g., by unbalanced rotating machinery or traveling vehicles, can lead to dynamic instability in the form of parametric resonance (Rayleigh, 1894). The structure moves in such a way that the axial mode absorbs an unbounded amount of energy from the load. This kind of resonance occurs at double the natural frequency of lateral vibrations corresponding to the static (average) value of the load (Figure 1(c)). The doubling of frequency is explained by the fact that the second-order axial (or in-plane) strains due to lateral deflections of columns (or plates), on which the axial (or in-plane) forces work, have double the frequency of the lateral deflections.
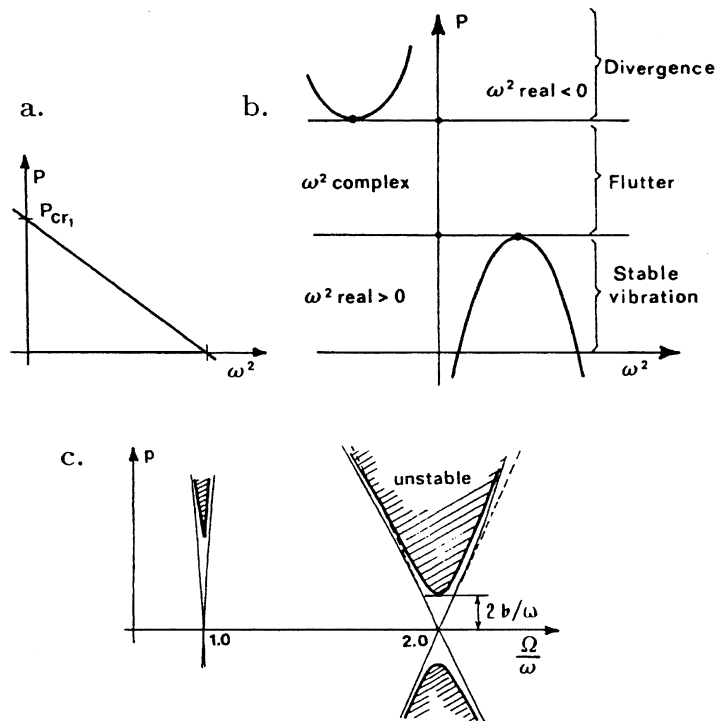
Figure 1 (a) Dependence of free vibration frequency ω on static load P for conservative systems. (b) Typical example for nonconservative systems. (c) Strutt diagram for parametric resonance (p = amplitude parameter of pulsating load; Ω = forcing frequency; b = damping parameter).

Due to higher-order Fourier components of axial strain history, a milder parametric resonance may also occur at other integer multiples of the natural frequency. An important aspect of parametric resonance is that the structure is stabilized by sufficient damping. In conservative systems, by contrast, the damping has no stabilizing influence.

In a rotating coordinate system, forces resulting from apparent accelerations, such as the Coriolis force and gyroscopic moments, can stabilize the structure even though they do no work on the motion of the structure. The Coriolis force, e.g., causes an unbalanced rotating shaft to regain stability at supercritical rotation velocities.

An important consequence of Liapunov's definition of stability is the Lagrange–Dirichlet theorem (Lagrange, 1788). When the total energy is continuous and all the forces are conservative or dissipative, the equilibrium is stable if the potential energy of the structure as a function of all the generalized displacements is positive definite (i.e., has a strict minimum).

This theorem greatly simplifies the analysis of conservative systems, making it possible to use static analysis, avoiding the complications of dynamic analysis of a structure with symmetry-breaking imperfections. To simplify the analysis of nonconservative systems, it is of

great interest to find test functions analogous to potential energy, called Liapunov functions, which make it possible to decide stability without dynamic analysis. Such functions, however, have been discovered only for some special situations with nonconservative loads.

Nonlinear dynamic systems that cannot be linearized can exhibit a complex dynamic response that is nonperiodic and appears to be random (Figure 2). Such a response, called chaos, shows nevertheless a certain degree of order and cannot be described by methods of random dynamics. Great attention has been devoted to the trajectories of response of such systems in the phase space (a space whose coordinates are the generalized displacements and their velocities). A typical property of damped stable linear oscillators is that the trajectory is attracted, in several characteristic ways, to a single point, called the attractor. For a nonlinear oscillator, the trajectory appears as chaotic but, on closer scrutiny, is often found to be attracted to something called the 'strange attractor', which describes a hidden order in the response and normally has a fractal structure. Chaotic systems are inherently unstable—very small perturbations produce trajectories that exponentially diverge from the original trajectory (Figure 2). This makes the response over longer periods of time unpre-
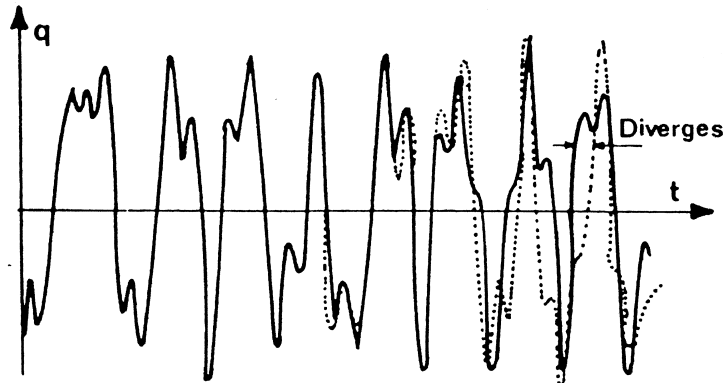
Figure 2 Chaotic vibration of nonlinear system (divergent response change caused by a very small change in initial conditions).

dictable (Thompson, 1982, 1989; Thompson and Stewart, 1986; Moon, 1986).

2.02.2.3 Energy Analysis of Stability of Elastic Structures, Postcritical Behavior, and Catastrophe Theory

By virtue of the Lagrange–Dirichlet theorem, stability of equilibrium of elastic structures under conservative loads can be decided by checking the positive definiteness (existence of a strict minimum) of the potential energy Π as a function of displacement vector q near the minimum point of Π. Aside from q, Π also depends on various control parameters including load P and, for imperfect structures, also on the imperfection magnitude α characterizing the deviation from symmetry.

The Taylor series expansion of the potential energy in terms of displacement vector q about the equilibrium state (defined as $q = 0$) begins with the quadratic term called the second variation,

$$\delta^2 \Pi = \frac{q^{\mathrm{T}} K q}{2} \tag{4}$$

where

$$K = \frac{\partial^2 \Pi}{\partial q^{\mathrm{T}} \partial q} \tag{5}$$

which represents the tangential stiffness matrix. The structure is stable if $\delta^2 \Pi$ (or K) is positive definite. If the potential exists, K is symmetric (and real), and so the structure is stable if and only if all the eigenvalues of K are positive; or equivalently, if and only if all the principal minors of K are positive (Sylvester's criterion).

Of main interest is the lowest critical load, $P = P_{\mathrm{cr1}}$, for which K becomes singular and the quadratic form $\delta^2 \Pi$ positive semidefinite. For columns and frames (but not necessarily plates
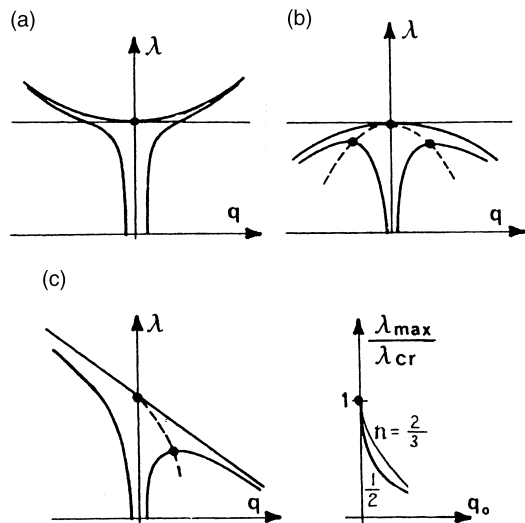
Figure 3 Responses of perfect and imperfect structures in bifurcation buckling: (a) stable symmetric, (b) unstable symmetric, (c) asymmetric, and (right) Koiter's power laws (λ = load parameter, q = lateral deflection, $q_0 = q$ at $\lambda_{\max}$).

and shells), the lowest critical load is the first, for which the buckling wavelength is the longest. In conservative systems, the lowest critical load represents the limit of stability. For higher loads P, the quadratic form is indefinite or negative definite, which implies that conservative systems are unstable for $P > P_{\mathrm{cr1}}$.

The behavior after the critical load is reached, called the postcritical behavior (Figure 3), is determined by the term of the Taylor series expansion of Π that comes next after the quadratic term. An important aspect is the postcritical imperfection sensitivity, which describes how the maximum load, $P_{\max}$, is affected by the magnitude of small imperfection α. Despite tremendous variety of structural forms, all the initial postcritical behavior can take only a few typical forms.

For many structures, Π can be considered a function of only one deflection parameter q. Typical are symmetric structures which, in the absence of imperfections, remain symmetric up to the lowest critical load P_{cr}. They possess a potential energy function $\Pi(q)$ that contains the quadratic and quartic terms but misses the cubic terms in the Taylor series expansion. Such structures exhibit postcritical behavior that is symmetric with respect to q, termed symmetric bifurcation. Depending on the sign of the quartic term, the critical state may be stable or unstable, which is called the stable or unstable symmetric bifurcation (Figures 3(a) and (b)). The former (which is typical of columns, symmetric frames, and plates) is imperfection insensitive. The latter is imperfection sensitive (a behavior found is some types of frames; Bažant and Cedolin, 1991; Bažant and Xiang, 1997a); this means that the equilibrium load value of perfect structure ($\alpha = 0$) decreases with $|q|$, and that $P_{max} < p_{cr}$ for $\alpha \neq 0$.

Imperfection sensitivity, i.e. the reduction of P_{max} caused by imperfection, is stronger for elastic structures that exhibit bifurcation and possess the cubic terms in $\Pi(q)$. In that case, which is called asymmetric bifurcation, the critical state is always unstable and the structure is always imperfection sensitive (Figures 3(c), 4). Such behavior is typically exhibited by asymmetric frames (the classical example being the Γ-shaped frame; Figure 4),
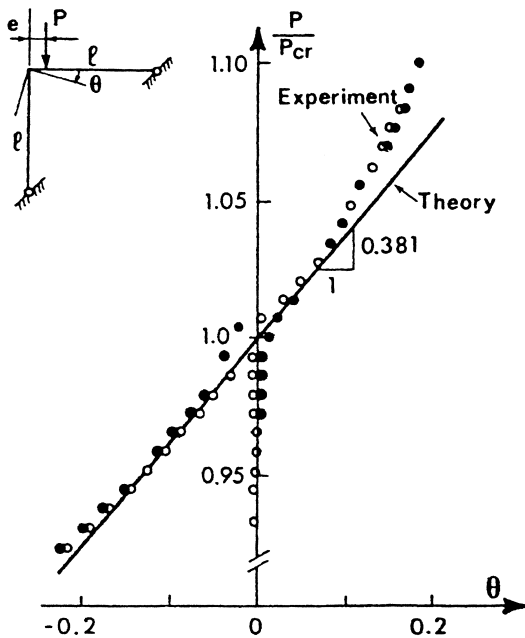
and in an extreme manner by many shells (e.g., spherical shells, or cylindrical shells under axial compression or bending (but not under radial pressure or torsion)).

A famous result of elastic stability theory is that, for all types of imperfection sensitive elastic structures, the postcritical imperfection sensitivity of bifurcation buckling can be only of two types, characterized by Koiter's (1945) power laws:

$$\frac{\Delta P_{max}}{P_{cr}} \propto \alpha^{2/3} \text{ or } \alpha^{1/2} \qquad (6)$$

where $\Delta P_{max} = P_{cr} - P_{max}$. The former applies to unstable symmetric bifurcation, and the latter to asymmetric bifurcation. The latter is generally more dangerous because ΔP_{max} is much larger when α is sufficiently small. Imperfection sensitivity is also important for dynamic buckling (Budiansky and Hutchinson, 1964).

Consider now elastic structures that possess no cubic term in $\Pi(q)$ and exhibit no bifurcation, due to nonexistence of symmetric deflections. In this case, called snapthrough, the deflection curve $P(q)$ has a limit point (peak, maximum point, P_{max}), which represents the stability limit (critical state) if the load is a gravity load (dead load). After the limit point, the response under gravity load becomes dynamic; the structure 'snaps through', in accelerated motion. Such behavior is typical of flat arches or shallow (cylindrical or spherical) shells, in which the failure is caused by shortening of the arch or in-plane normal strains of the shell. The postpeak equilibrium load-deflection curve exhibits postpeak softening, which is unstable for load control (gravity load). For displacement control, the postpeak softening is stable, but only as long as the slope of the curve is negative. If the slope becomes vertical, stability is lost despite displacement control, which is called snapdown. After snapdown, the slope of the curve may become positive again but the states are unstable. Snapdown is exhibited by elastic flat arches or shallow shells loaded through a sufficiently soft spring.

In bifurcation buckling, the deflection curves of imperfect structures exhibit a limit point with snapthrough rather than bifurcation. Since inevitably some imperfections are always present, bifurcation buckling is merely an abstraction, albeit a very useful one.

When a structure has two equal or nearly equal critical loads corresponding to different buckling modes, the modes usually interact in a way to cause imperfection sensitivity. This occurs in built-up (latticed) columns if the

Figure 4 Roorda's (1971) experimental verification of calculated postcritical response in asymmetric bifurcation of a Γ-frame.

flanges or lattice members buckle locally at the same load as the column as a whole, in stiffened plate girders if the stiffening ribs buckle locally at the same load as the web, in box girders if the stiffeners buckle locally at the same load as the plates, or if the plates buckle at the same load as the box, etc. Disregarding postcritical behavior, designs with coincident critical modes would seem to yield optimum weight, but in fact they represent what is called the "naive" optimal design, which must be avoided because it produces high imperfection sensitivity.

The type of buckling of a system governed by a potential is qualitatively fully determined by the topological characteristics of the potential surface. The problem is analogous to instabilities encountered in various fields of physics and other sciences and is generally described by the catastrophe theory. Consider the potential Π as a general function of free variables $q_1, \ldots, q_n$, and of control parameters $\lambda_1, \ldots, \lambda_m$ corresponding to the load and the imperfections. If $n = m = 1$, there exists only one type of catastrophe called the fold, equivalent to snapthrough or to asymmetric bifurcation. If $n = 1$ and $m \le 2$, there exists a second catastrophe called the cusp, equivalent to symmetric bifurcation (Figure 5). If $n \le 2$ and $m \le 4$, there exist seven catastrophes, the five additional ones being called the swallow-tail, butterfly, hyperbolic umbilic, elliptic umbilic, parabolic umbilic, and double cusp (this remarkable result has been rigorously proved by Thom, 1975). Examples of elastic structures that exhibit all these seven catastrophes have been given, although some have an air of artificiality. Completely general though the catastrophe theory is usually perceived to be, its present form is nevertheless inapplicable to elastoplastic, damaging and fracturing structures—a very important class.

The potential energy concept is useful as the basis of direct variational methods of calculating the critical loads of continuous elastic structures. The deflection field is described as

$$w(\boldsymbol{x}) = \sum_{i=n}^{\infty} q_i \phi_i(\boldsymbol{x}) \qquad (7)$$

where $\phi_i(\boldsymbol{x})$ are chosen as linearly independent (preferably orthogonal) functions of the coordinate vector $\boldsymbol{x}$ (1D, 2D, or 3D). In the Ritz (or Rayleigh–Ritz) variational method, the potential energy Π is minimized with respect to deflection parameters q_i. This yields the necessary conditions

$$\frac{\partial \Pi}{\partial q_i} = 0 \qquad (8)$$
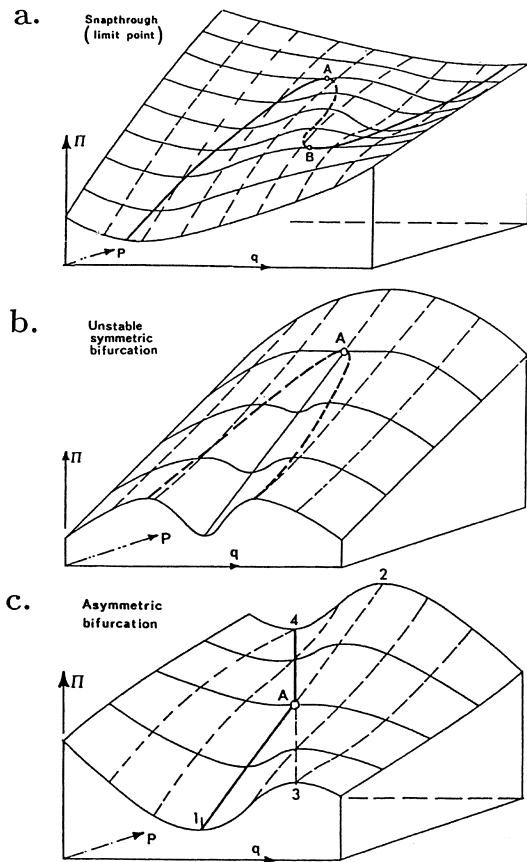
Figure 5 Surfaces of potential Π for three buckling types. (a) Snapthrough or limit point (fold catastrophe). (b) Unstable symmetric bifurcation (cusp catastrophe). (c) Asymmetric bifurcation (also fold catastrophe); q = deflection, $P = \lambda$ = load parameter.

for all q_i, which represent equations for q_i. If Π is quadratic, the equations are linear, and if they are homogeneous one has a matrix eigenvalue problem for the critical load. The solution converges for $n \to \infty$ if functions $\phi_i(\boldsymbol{x})$ form a complete system. For a finite n, one has an upper bound approximation on P_{cr1}, which is close enough if n is large enough or if the selected functions $\phi_i(\boldsymbol{x})$ can closely approximate the deflection shape. The FE method for conservative problems can be regarded as a special case of the Ritz variational method.

Often it suffices to use only one judiciously chosen function $\phi_1(\boldsymbol{x})$; the critical load is then given by the Rayleigh (1894) quotient

$$P_{\mathrm{R}} = \frac{U}{\overline{W}} \qquad (9)$$

where U = strain-energy expression (quadratic) in terms of displacement distribution, w, and $\overline{W}$ = expression for work per unit load, $P = 1$ (also quadratic). Analyzing $\delta^2 P_{\mathrm{R}}$, one can

prove that P_R represents an upper bound on P_{cr1}. The Ritz method is equivalent to minimization of P_R with respect to $\phi_1(x)$ (considered as unknown). In mathematics, the Rayleigh quotient P_R is equivalently expressed in terms of the differential operators of the boundary value problem (provided the problem is self-adjoint, which is automatically the case if Π exists).

For statically determinate columns, an upper bound that is always closer to P_{cr1} than P_R is given by the Timoshenko quotient

$$P_T = \frac{\bar{W}}{U_1} \qquad (10)$$

where U_1 is the complementary strain energy calculated from the second-order bending moments M caused by a unit load ($P = 1$) acting on the deflections w, expressed in terms of w. P_T can be shown to represent nothing else but the Rayleigh quotient as defined in mathematics on the basis of the differential operators of the second-order differential equation for buckling of statically determinate columns.

From the viewpoint of design safety, it would be preferable to have lower bounds rather than upper bounds on P_{cr1}; they exist but, unfortunately, in most cases are not close enough to be useful (Bažant and Cedolin, 1991, section 5.8).

Based on the calculus of variations, from Π as a functional of deflection $w(x)$, one can derive the differential equation of the problem. This approach, which is useful for more complicated problems such as thin-wall bars, also yields the boundary conditions that are compatible with the existence of a potential. They are of two kinds: kinematic (essential) or static (natural).

### 2.02.2.4 Shells, Plates, Thin-wall Beams, and Sandwiches

The design of shells and plates is dominated by stability. Shell buckling is a problem with a fascinating history. After the critical loads of externally pressurized spherical shells and axially compressed cylindrical shells were calculated at the dawn of the twentieth century (Lorenz, 1908; Timoshenko, 1910; Southwell, 1914), they were found to be 3–8 times larger than the experimental failure loads (Figure 6(b)). Despite persistent efforts, the discrepancy remained unexplained until von Kármán and Tsien (1941) (Figure 6(a)) discovered the answer to lie in the extreme imperfection sensitivity of nonlinear postcritical behavior which causes the bifurcation to be asymmetric (their celebrated result was later found to fit the

broader context of Koiter's (1945) postcritical theory, already discussed). The asymmetry is caused by the fact that the radial resultant of the in-plane stresses in a curved shell has a deflection-dependent quadratic term which resists an inward buckle and assists an outward buckle (this resultant is analogous to a nonlinear quadratic lateral spring support of a column; von Kármán and Tsien, 1941).

The buckling of some shells is imperfection insensitive, permitting the design to be based on critical loads (e.g., a cylindrical shell subjected to lateral pressure or torsion; Figure 6(c)). The archetypical cases of imperfection-sensitive shells are the externally pressurized spherical shell and the cylindrical shell subjected to axial compression or bending. In theory, a perfect shell of the imperfection-sensitive type exhibits, after bifurcation, a dynamic snapdown to a postcritical load value typically equal to only 15–35% of P_{cr1}, but in practice the imperfections are always so large that the load cannot exceed these values at reasonable deflections (see the curves for imperfection parameter 0.1 or 0.2 in Figure 6(a)). That the critical loads can indeed be closely approached was experimentally demonstrated only when Almroth *et al.* (1964) and Tennyson (1969) succeeded in fabricating cylindrical shells with extraordinarily small imperfections.

The critical loads for axisymmetric buckling (Figure 6(d), bottom) represent a 1D problem which can be solved easily. The 2D non-axisymmetric buckling modes (Figure 6(d), top) are harder to solve. Often the problem can be simplified by considering the shell as shallow (which means that the rise of every possible buckle is small compared to the chord of the buckle arc). A famous result for such shells was Donnell's (1934) reduction of the critical load problem to one linearized eighth-order partial differential equation for shell deflection. A system of eight linearized partial differential equations, known as the Donnell–Mushtari–Vlasov theory, was obtained for general shallow shells. Based on the shallow shell approximation, critical loads for many modes of various shells have been solved analytically, before the FE era.

Calculation of the postcritical behavior and failure loads of shells is a difficult problem, sometimes even with FE programs. Although verification of an important design by FEs is imperative, the design is generally based on critical load solutions reduced by an empirical "knock-down" factor ϕ which accounts for imperfection sensitivity and has been tabulated for various practical cases (e.g., Kollár and Dulácska 1984). For instance, for a cylindrical
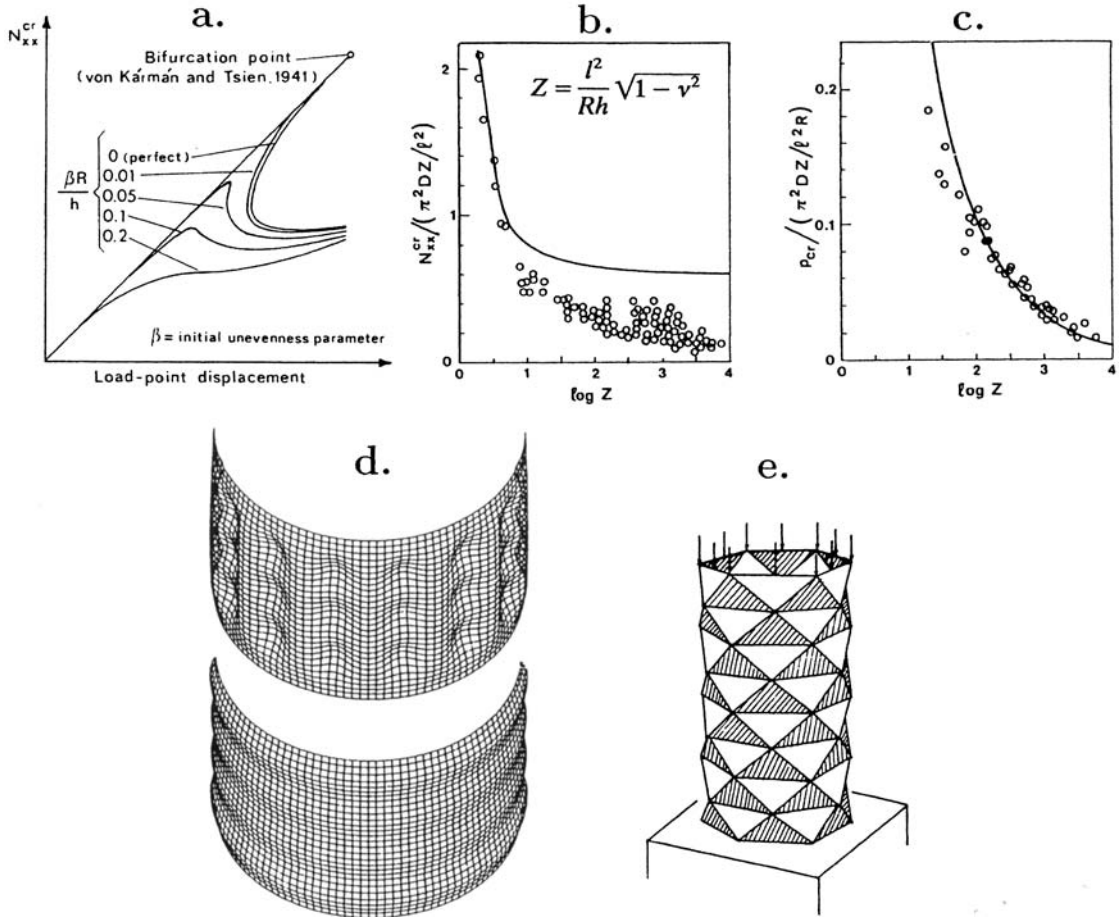
Figure 6 (a) Von Kármán and Tsien's (1941) postcritical diagrams of axial compression force versus shortening of cylindrical shell. (b) and (c) Comparison of critical loads of perfect shells with measured failure loads for cylindrical shells under axial compression (b) or radial pressure (c) (R, h, l = radius, thickness and length of shell). (d) Critical modes. (e) Yoshimura's final buckle pattern.

shell of radius R and thickness h, the axial internal force at failure is expressed as

$$N_{xx}^* = \frac{\phi E h^2}{R\sqrt{3(1-v^2)}} \qquad (11)$$

where v = Poisson's ratio, and ϕ depends on R/h (e.g., Budiansky and Hutchinson, 1972; Budiansky, 1974). For combined loadings, a linear interaction diagram may be safely assumed in design (as, e.g., between the maximum N_{xx} values due to bending and to axial loading of a cylindrical shell). Because the imperfections are highly random and have a large influence, a probabilistic estimation of the failure load is appropriate (e.g. Bolotin, 1969).

The reason for the extreme imperfection sensitivity of shells may be seen in the existence of many buckling modes with nearly equal critical stresses. For example, the critical stresses for many nonaxisymmetric buckling modes of an axially compressed cylindrical shell are only slightly lower than that for the axisymmetric pattern. In postcritical deflections, the buckle patterns may change and the final one is the diamond buckle pattern (Yoshimura pattern, Figure 6(e)). When a significant lateral pressure is superimposed on axial compression, the critical loads for different modes are no longer close to each other, and such a shell ceases to be imperfection sensitive.

Some nonlinear problems of shells were approximately solved before the advent of FEs (e.g., by variational series expansions). Many older analytical solutions, however, have now lost much of their value because of their complexity. But those that are simple nevertheless remain valuable for the understanding they convey and for use as checks on FE codes, and are invaluable for design optimization and probabilistic modeling.

Let us now discuss the simpler problem of plates, which became well understood about two decades earlier than shells. Fourier series with Ritz variational methods were used before

the middle of the twentieth century to solve the critical loads of rectangular or circular plates with various edge conditions and diverse combinations of in-plane normal and shear forces (e.g. Timoshenko and Gere, 1961). Like shells, plates exhibit many buckling modes. Unlike shells, the critical loads are far apart (and thus they cannot interact to cause imperfection sensitivity). In contrast to columns and in similarity to shells, the critical mode with the longest wavelength in one direction is not necessarily the lowest critical load for plates.

In contrast to shells, the buckling of plates is not imperfection sensitive. This was established early in the nineteenth century on the basis of the approximate solutions of the famous von Kármán (1910)–Föppl (1907) nonlinear equations for initial postcritical behavior (two coupled fourth-order partial differential equations for the deflection and the Airy stress function of in-plane stresses). If large deflections take place, plates supported along their entire boundary show a substantial postcritical reserve. Its source is the ability of a plate to redistribute the in-plane compressive forces into compressed cylindrically buckled strips along the boundaries (for compression parallel to supported edges) and into diagonal tensioned strips (for shear loading). When large buckles develop and the cylindrically buckled strips carry most of the in-plane forces, the plate acts essentially as a truss. Ultimately, the buckled strips yield, which means that simple limit analysis can be applied to the truss. Such a truss analogy was exploited by von Kármán *et al.* (1932) to deduce stunningly simple approximate formulas for the maximum postcritical load $P_{\max}$ of plates subjected to compression and shear; for simply supported rectangular plates compressed in the direction of one side,

$$P_{\max} \approx kh^2\sqrt{E\sigma_{\mathrm{Y}}} \qquad (12)$$

which, remarkably, does not depend on the plate dimensions ($h =$ plate thickness, $\sigma_{\mathrm{Y}} =$ yield stress, and $k \approx$ constant).

Transverse shear deformations are unimportant in thin plates and shells. But they may be significant in composite shells, and dominate the buckling of sandwich plates and shells (e.g., Plantema, 1966), i.e., plates that consist of stiff but thin face sheets (skins) bonded to a soft core (a foam or honeycomb). Local buckling of the skin, which provokes delamination fracture, is an additional very important mode of instability of sandwiches. In sandwich shells, the critical loads for axisymmetric buckling modes and modes with periodic buckles along

the circumference are distinctly separated, which suppresses postcritical imperfection sensitivity (Tennyson and Chan, 1990). Microbuckling of fibers due to shear causes compressive kink-band failure in composites (Rosen, 1965; Budiansky, 1983; Fleck, 1997; Bažant *et al.*, 1999).

Long thin-wall girders (e.g., metallic cold-formed profiles, concrete or welded steel girders for large bridges and buildings) represent long shells that can be approximately treated according to the theory of thin-wall beams. The first important result in this broad domain was contributed by Prandtl (1899) in his dissertation on lateral buckling of beams of rectangular cross section subjected to bending, which he obtained in terms of Bessel functions and verified by his experiments. His pioneering work, as well as the simultaneous solution of a special case of lateral buckling by Michell (1899), stimulated rapid further progress.

The theory of thin-wall beams can in general be regarded as a semi-variational approach (Kantorovich variational method) in which the basic modes of deformation in the transverse directions are judiciously assumed and energy minimization then yields ordinary differential equations for the deflections and torsional rotations as well as the parameters of these modes as functions of the longitudinal coordinate. The reduction of the problem to ordinary differential equations greatly simplifies stability analysis. Beside the deformation modes described by Saint-Venant torsion theory and by the theory of bending with plane cross sections, one must consider for beams of open profile a mode in which the cross section warps out of plane. The bimoment produced by the warping mode is an important mechanism in resisting torsion (the resistance being provided by axial normal stresses characterized by the bimoment). In box girders, one must also include modes describing the bending deformation of the cross section within its own plane. 1D FEs of thin-wall beams of open or closed cross section, incorporating the out-of-plane warping mode and the in-plane cross-section deformation mode, have been formulated and used to analyze critical loads and postcritical behavior.

Solutions based on the warping torsion theory describe the important cases of lateral buckling of thin-wall beams, in which a horizontal beam subjected to bending in the vertical plane twists and bends laterally, and of axial-torsional buckling of an axially compressed column.

Limited though the studies of postcritical behavior have been, some FE studies indicate that lateral buckling of beams is not

imperfection sensitive and has a high post-critical reserve.

2.02.3 ANELASTIC AND DISINTEGRATING STRUCTURES

2.02.3.1 Elastoplastic Buckling and Shanley's Bifurcation

Elastic structures fail either by exhausting material strength or by instability. Structures that are not elastic may, and usually do, fail by a combination of both. The evolution of material failure becomes a part of process of stability loss of the structure. Consideration of inelastic behavior and material failure is today an essential ingredient of a sound assessment of stability of structures.

A salient property of elastoplastic behavior is the irreversibility at unloading, manifested by the fact that the unloading modulus E_u is larger that the tangent modulus E_t for further loading (in absence of damage, $E_u = E$). This property causes a type of behavior not seen in elastic structures: the bifurcation of equilibrium path in the load-deflection space can, and in fact does, occur at increasing, rather than constant, load P. This phenomenon was discovered by Shanley (1947) in a revolutionizing paper which corrected a previous erroneous concept that had lasted over half a century.

The problem has a complicated history. In two subsequent studies, Engesser (1889, 1895) proposed two different formulas for the load at which a perfect elastoplastic column begins to buckle:

$$P_t = \frac{\pi^2}{L^2} E_t I \quad \text{or} \quad P_r = \frac{\pi^2}{L^2} E_r I \qquad (13)$$

where P_t is called the tangent modulus load, and P_r the reduced modulus load (Figure 7(a)); E_t is the tangent modulus of material for further loading from the stress level at initial unbuckled state, and the reduced modulus E_r (dependent on cross section geometry; Engesser, 1895, 1898) is calculated as the effective modulus for buckling at constant load (for which E_t applies at the side of neutral axis that undergoes further shortening, while E_u applies at the side that undergoes extension (unloading) during deflection). The reduced modulus theory, yielding P_r, was supported and refined by von Kármán (1910). It had been accepted as valid for five decades, until tests on aluminum alloys and high strength steels, exhibiting a slowly decreasing E_t, revealed the buckling to begin at P_t, which can be much smaller than P_r.

Based on Shanley's (1947) epoch-making discovery, which was immediately accepted by von Kármán and was later generalized to 3D solids by Hill (1962) and others, the first bifurcation of the equilibrium load-deflection path (Figure 7(a)) occurs when the tangential stiffness matrix K_t of the structure becomes singular or, in the case of a discontinuous evolution of E_t, when the smallest eigenvalue of K_t jumps from positive to negative (the reason will be mentioned later, in Equation (21)). No unloading occurs anywhere in the structure, and the analysis based on K_t is often called Hill's (1962) method of linear comparison solid. This is a valuable simplification. However, the problem of bifurcation load is still nonlinear because E_t depends on P_t as described by the elastoplastic constitutive law.

In contrast to elastic bifurcation, the Shanley first bifurcation state does not represent neutral equilibrium; the initial postbifurcation states are always stable. The symmetry-breaking secondary path (i.e., lateral deflection) is nevertheless the path that must occur in reality. These facts can be proved either by analysis of imperfections or, less tediously and more generally, by calculating the second variation $\delta^2 S$ of the entropy increment (or Helmholtz free energy increment) of a perfect structure and the differences in entropy increment between the primary and secondary paths (Bažant and Cedolin, 1991, section 10.2; Figure 7(b)).

In an elastoplastic column, all the (infinitely many) undeflected states between P_t and P_r represent bifurcation states (Figure 7(a)). They are stable if the load is controlled, and P_r is the stability limit. If the load-point displacement is controlled, the stability limit is higher than P_r. The maximum load, P_{max}, is in practice usually much closer to P_t than to P_r (Figure 7(a)). It is for this reason that P_t is so important. The design of metallic columns, frames, thin-wall beams and shells is now generally based on the tangential modulus, and the concept is also valid for concrete (Bažant and Cedolin, 1991; Bažant and Xiang, 1997b).

The initial postbifurcation behavior of perfect and imperfect structures near P_t is stable. In contrast to elastic structures, the deflections to the right and left are not symmetric if the cross section is nonsymmetric, and the P_r and P_{max} values for buckling to opposite sides are different.

When E_t as a function of stress drops suddenly, which occurs for mild steel, P_r can, and normally does, coincide with P_t. In this light, it might seem strange that tests of hot-rolled steel profiles made of mild steel exhibit a large difference between P_r and P_t. The reason is that very large residual thermal stresses get locked in after initial cooling in the steel mill
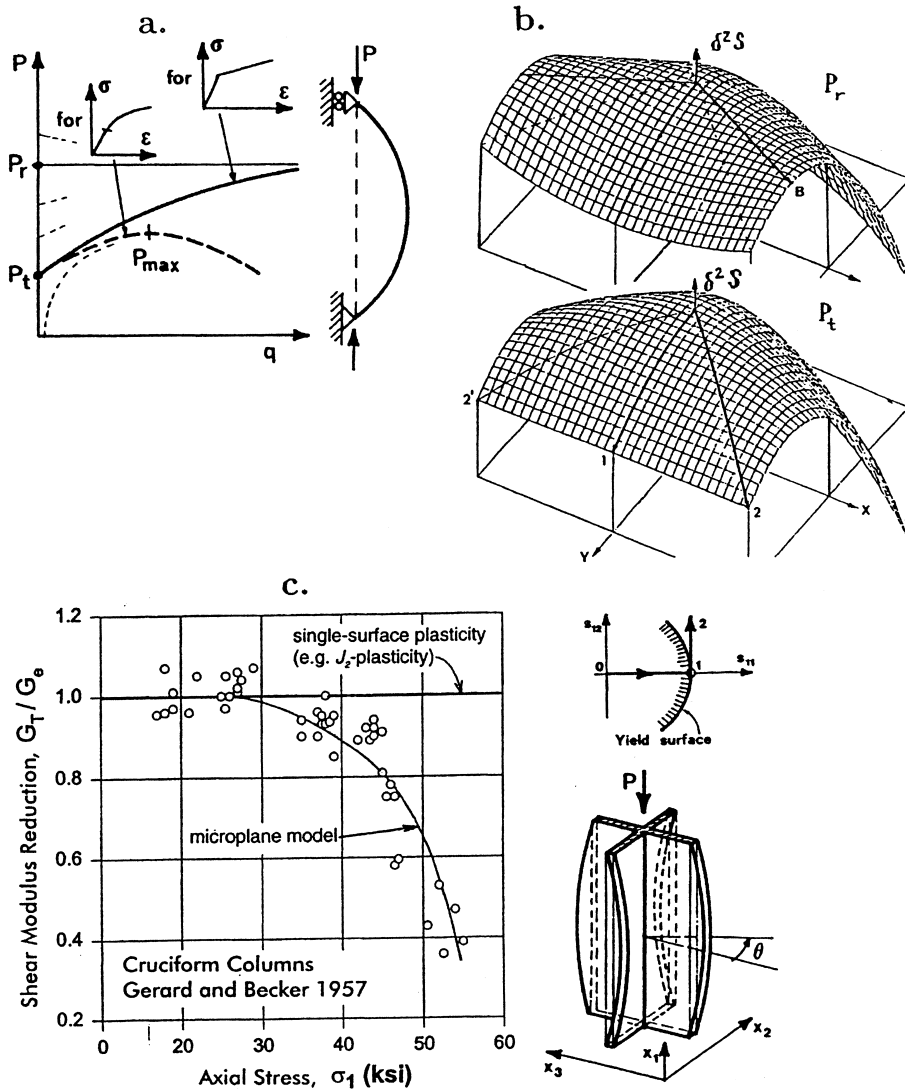
Figure 7 Inelastic buckling. (a) Shanley bifurcation in plastic structures with a smooth or bilinear stress–strain diagram. (b) Corresponding surfaces of the second variation of entropy $\delta^2 S$ (the negative of potential $\delta^2 \mathcal{F}$) at Shanley bifurcation (bottom) and at reduced modulus load (top). (c) Reduction of tangential shear modulus derived from torsional critical loads of axially compressed elastic-plastic cruciform columns measured by Gerard and Becker (1957), and comparison with (smoothed) results of microplane model for steel (solid curve, Brocca and Bažant, 2000).

(Osgood 1951; Yang *et al.* 1952). They cause the cross-section parts with different residual stresses to begin yielding at very different load values, thus rendering the overall force–deformation diagrams of the cross section smoothly curved. Discovery of this phenomenon resolved several previous decades of groping in efforts to explain the experiments in terms of imperfections alone. Thus Shanley's theory is important not only for alloy steels but also for hot-rolled profiles made of low-carbon mild steel which passes from elastic behavior to perfectly plastic yielding almost instantly.

The buckling behavior of reinforced concrete columns is complicated by tensile cracking.

Young's formula for the effect of imperfections on the deflection and moment magnification is used in design, complemented by an empirical formula for the effective modulus. The magnified moment M and axial force P are then compared to a semi-empirical strength envelope in the (P, M) plane. Consideration of perfect columns is avoided by prescribing for consideration in design a certain minimum load eccentricity (Figure 8).

Our discussion so far pertains to small deflection behavior. Large plastic deflections of columns are of interest mainly for predicting the energy absorption capability under blast, impact, and earthquake. If the yield plateau of
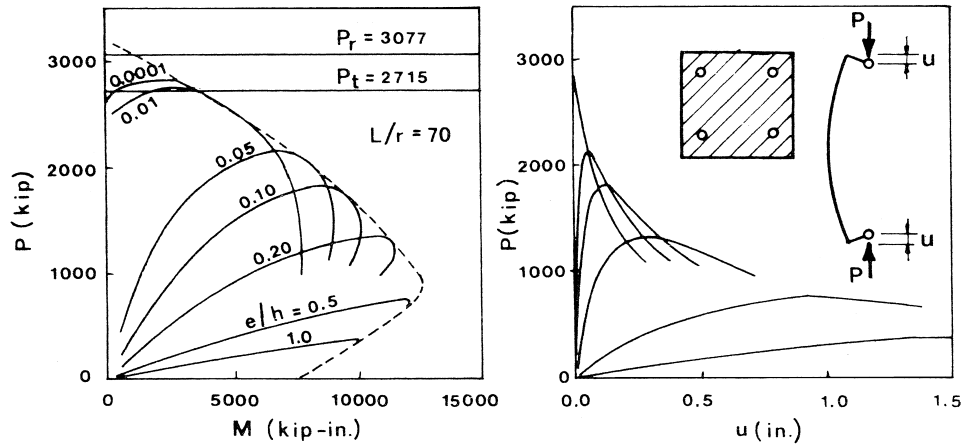
Figure 8   Left: typical failure envelope (interaction diagram) and curves of axial load P versus maximum bending moment M for a reinforced concrete column of slenderness $L/r = 70$, loaded at various constant relative load eccentricities e/h (P = load in 1000 lb., M = maximum bending moment in 1000 lb × in.). Right: corresponding diagrams of P versus axial displacement u.

the material is long enough, the fully plastic softening postpeak response of columns and frames can be determined relatively easily by analyzing a plastic hinge mechanism subjected to axial forces. When the structure is slender and has high initial bending moments or large imperfections, which is often the case, the transition from elastic behavior to the hinge mechanism is so rapid that it may be considered as sudden. A close upper bound for the energy absorption capability of the structure is then provided by the area under the load-deflection curves for elastic behavior and for the plastic hinge mechanism. The intersection of these curves is an upper bound on the maximum load (provided the elastic load-deflection curve is rising up to the intersection). In the case of buckling of thin plastic plates under in-plane forces, one may similarly base a simple calculation on a yield line mechanism.

Very difficult 3D problems are the plastic localization instabilities caused by the geometrically nonlinear effects of finite strain (Rudnicki and Rice 1975; Bažant and Cedolin, 1991, chap. 13). The best known example is necking (e.g., Hutchinson and Neale, 1978)—a narrowing of the cross section of a bar that is initially under uniform tensile strain. The narrowing causes the load to peak and then decrease at increasing displacement. Finite-strain FE solutions (e.g., Needleman, 1982; Tvergaard, 1982) are very sensitive to the precise form of the plastic constitutive law. Geometric nonlinearity, however, is not the only cause of necking. A complete analysis needs to take into account also the damage due to the growth of voids or microcracks (which is discussed in a later section).

Analysis of plastic localization instabilities is required to understand the bursting of pipes and other shells caused by internal pressure, bending failure of tubes due to ovalization of cross-section, postcritical reserve in plates and thin-wall beams, etc.

2.02.3.2   Stability Implications of Normality Rule and Vertex Effect

When multiaxial stresses and strains arise in buckling, a strong sensitivity to the multiaxial nature of the elastoplastic constitutive law is encountered. A central concept in the formulation of these laws is the normality rule. This rule requires that, in the 9D spaces of the components of the stress tensor and the strain rate tensor, the strain rate (plastic flow) vector must be normal to the current yield surface. A special form of the normality rule, in the context of the J_2 flow theory, was proposed by Prandtl (1924). Later, the normality rule was generalized for any type of yield surface and was derived from certain plausible work inequalities (Hill, 1950; Drucker, 1951). It was recognized that adherence to this rule, originated by Prandtl, is essential (Drucker, 1951; Rice, 1971) for ensuring stability of the material, particularly for preventing spurious strain localization instabilities (to be discussed later).

Various experimentally observed phenomena such as the dilatancy of frictional slip were later found to be in apparent violation of the normality rule. One such phenomenon, the so-called vertex effect, was brought to light by Gerard and Becker's (1957) tests of torsional buckling of short axially compressed thin-wall

cruciform columns (Figure 7(c)). The bifurcation load of these columns is proportional to the incremental material stiffness "to-the-side," i.e., the stiffness (in this case the shear modulus) for a stress increment vector that is tangential to the yield surface in the 9D space of stress components (top right in Figure 7(c)). According to the classical J_2-plasticity theory based on the normality rule, as well as all the plasticity theories with a single loading potential surface in the deviatoric stress space, the stiffness "to-the-side" is equal to the initial elastic stiffness. Thus the critical load for torsional buckling of a cruciform column is predicted by these theories to be equal to the elastic critical load, regardless of the axial compressive stress. This is grossly incorrect and far higher than the measured values (Figure 7(c) left).

This inadequate performance of the plasticity models with a single loading potential in the deviatoric stress space, which, as of early 2000s, dominate the computational practice, has not been taken seriously for a long time, and has almost been forgotten in research without ever being satisfactorily resolved. Four theories that have been used to deal with this paramount problem of plasticity may be mentioned.

(i) Hencky's deformation theory of plasticity. It predicts the stiffness to-the-side to be secant stiffness, which can be much smaller than the initial elastic stiffness and gives a relatively good agreement with Gerard and Becker's buckling experiments. However, Hencky's is not a fully consistent theory suitable for general FE programs.

(ii) Enhancement of the plastic potential surface with a vertex traveling with the current stress point (Rice, 1975; Rudnicki and Rice, 1975; Hutchinson and Neale, 1978; Hutchinson and Tvergaard, 1980; Bažant, 1980; Bažant and Cedolin, 1991; section 10.7). This approach, however, does not seem effective for general FE programs.

(iii) Multisurface plasticity, proposed by Koiter (1953). This theory reflects the actual source of the vertex effect, which is due to an intersection of several loading potential surfaces at the current stress point. An important advantage of introducing multiple loading surfaces is that the vertex effect can be modeled even while the normality rule, crucially important for the soundness of constitutive laws (Rice, 1971), can be satisfied separately for the individual surfaces. The multisurface constitutive model, however, is hard to identify from test data and has not been developed for large-scale computations, partly because very many simultaneous loading surfaces would be required for a general model.

(iv) Taylor-type crystallographic models, initiated by Taylor (1938), worked out in detail first by Batdorf and Budianski (1949) and later refined by others, (e.g., Rice, 1971; Bronkhorst *et al.*, 1992; Hutchinson, 1970; Butler and McDowell, 1998), and the related microplane model (Bažant, 1984; Bažant and Planas, 1998, chap. 14; Carol and Bažant 1997; Brocca and Bažant, 2000; Caner and Bažant, 2000; Caner *et al.*, 2002). Both types of constitutive models are defined not in terms of tensors and their invariants but in terms of the stress and strain components on surfaces of various orientations in the material (called the microplanes for the latter type). Either the stress components (for Taylor models) or the strain components (for microplane models) are assumed to be the projections of the stress or strain tensor. These are essentially multisurface plasticity models, though not expressed in terms of tensors and their invariants. They can separately satisfy the normality rules, either on each crystallographic plane or on each microplane, yet exhibit the vertex behavior automatically, by describing its physical source directly. The microplane model, with efficient (optimal Gaussian) numerical integration over all spatial orientations of microplanes (Bažant and Oh, 1986), has been developed for large-scale computation of concrete and metals and has been shown (Brocca and Bažant, 2000) to automatically reproduce the inelastic buckling data for metals (Gerard and Becker, 1957) (see Figure 7(d)) as well as concrete (Caner *et al.*, 2002).

2.02.3.3 Viscoelastic and Viscoplastic Buckling

Viscoelastic or viscoplastic behavior dissipates energy, which does not destabilize a structure. Thus, according to the Lagrange–Dirichlet theorem, the stability limit of a viscoelastic structure must still be decided by the loss of positive definiteness of the potential for the elastic part of response. However, the stability limit is often not the issue of main practical interest. Rather, it is the maximum load for which the deflections and stresses during the desired lifetime remain tolerable, or the critical time for which the deflections and stresses under the given design load remain tolerable.

The differential or integral equations that govern viscoelastic buckling can be obtained from those that govern elastic buckling by replacing the elastic constants with the corresponding viscoelastic operator. This operator can be of a differential type, based on the Maxwell or Kelvin chain rheological model, or

of an integral type, corresponding to a continuous relaxation or retardation spectrum. If there is no aging, a Laplace transform can be used to reduce the problem to elastic buckling, and inversion of the Laplace transform then yields the time evolution of buckling deflections. For viscoelastic materials that are solids (i.e., do not possess a purely viscous response), a structure loaded to the stability limit takes an infinite time to develop a finite deflection as a result of an infinitesimal disturbance or imperfection (e.g., Freudenthal, 1950; Hilton, 1952). Therefore the long-time critical load, $P_{cr\infty}$, which is obtained by replacing the instantaneous elastic modulus E in the critical load solution with the long-time elastic modulus E_{∞}, is normally unimportant. Important for design is the time to reach, for given imperfections, the maximum tolerable deflection or the maximum (second-order) stress due to buckling. This time must not be less than the required design lifetime.

Viscoplastic buckling is different. In contrast to viscoelastic structures, there exists a finite critical timed t^* at which the deflection triggered by an infinitely small imperfection becomes finite (or the deflection triggered by a finite imperfection becomes infinite according to the geometrically linearized theory); e.g., Hoff (1958). The basis of design is to ensure that t^* exceeds the required lifetime. The higher the load, the smaller is t^*. If the viscoplastic material does not have a finite elastic limit (e.g., if the viscoplastic strain rate is a power function of stress magnitude), the critical load according to Liapunov's stability definition (implying an infinite load duration) is zero.

Long-time buckling of concrete structures is a very complicated but important phenomenon which has caused some slender columns and shells to collapse after many years of service. In the low (service) stress range, concrete is viscoelastic but exhibits aging, caused by chemical processes of hydration and by relaxation of micro-pre-stress induced by drying and chemical changes—processes going on for many years. The consequence is that the Volterra integral equation for strain history in terms of stress history has a nonconvolution kernel, and the discrete Kelvin or Maxwell chain model has age-dependent viscosities and elastic moduli. The aging makes the Laplace transform methods ineffective even in the viscoelastic range, but a numerical integration of the evolution of buckling response in time is easy. Simultaneous drying intensifies creep, and so the problem is coupled with diffusion processes. Furthermore, concrete undergoes cracking during buckling. This and the creep cause a gradual stress transfer from concrete to steel reinforcement. No wonder that crude empirical design procedures are still in use.

Detailed FE solutions that agree reasonably well with tests have nevertheless been achieved. The design of concrete columns relies on an empirical overconservative reduction of the effective elastic modulus, reflecting creep, aging and cracking (as well as the Shanley effect). For creep with aging, most effective is the use of the age-adjusted effective modulus method, which is based on a theorem stating that if the strain history is linearly dependent on the compliance function, then the stress history is linearly dependent on the corresponding relaxation function (Bažant and Cedolin, 1991).

Since the prediction of lifetime is rather uncertain, a statistical approach is appropriate.

2.02.3.4 Thermodynamics of Structures, Inelastic Stability, Bifurcation and Friction

So far our review of inelastic structures has not dealt with the problem of stability. Stability cannot, in principle, be based on elastic potential energy. This does not mean, however, that stability would have to be analyzed dynamically, according to Liapunov's stability criterion. An energy approach to stability, which is much simpler, can be based on thermodynamics of structure (Bažant and Cedolin, 1991) (a subject distinct from the thermodynamics of constitutive equations of materials).

According to Gibbs's form of the second law of thermodynamics, a thermodynamic system is stable if the entropy increment calculated for every admissible infinitesimal change of system state is negative. If this increment is zero for some change, the system is critical, and if it is positive for some change, the change must happen, which means that the initial equilibrium state of the system is unstable. This is a general thermodynamic definition of stability of equilibrium, which is equivalent to Liapunov's definition (except when dealing with stability of motion). Its beauty is that the analysis of the motion caused by initial imperfections, which can be rather laborious, may be skipped. It suffices to analyze the perfect structure, which is much simpler, especially if the structure is inelastic.

An inelastic structure is normally far from a state of thermodynamic equilibrium, at which all the dissipative processes would come to a standstill. In principle, this prohibits using classical thermodynamics, which deals only with states infinitely close to thermodynamic equilibrium. However, the use of irreversible

thermodynamics would cause great complication. It can fortunately be circumvented by the hypothesis of a tangentially equivalent inelastic structure (Bažant and Cedolin, 1991). This is a structure characterized by the tangential moduli, assumed to behave equivalently to the actual inelastic structure for small changes of state. The existence of such a structure is of course tacitly implied whenever the load increment in a computer program is analyzed on the basis of the tangent elastic modulus. At each stage of loading, there are many tangentially equivalent elastic structures corresponding to various possible combinations of tangential moduli for loading and unloading in various parts of the structures. In theory, they all need to be considered.

The deformations of elastic structures are reversible changes of state, and thus they do not change the entropy of the structure. However, the thermodynamic system must include the load, whose changes are defined independently of the equilibrium of the structure. For example, if the structure is in equilibrium under gravity loads P at initial deflections q_0, and its deflections q are then changed by δq away from equilibrium, the equilibrium values of the reactions $f(q)$ change but P does not. The disequilibrium creates entropy change

$$\Delta S = \int [P - f(q)]^{\mathrm{T}} \mathrm{d}q \qquad (14)$$

Substituting

$$f(q) \approx P + K_{\mathrm{t}}(q - q_0) \qquad (15)$$

and integrating from q_0 to $q_0 + \delta q$, one has

$$-T\Delta S = \delta^2 W = \tfrac{1}{2}\delta q^{\mathrm{T}} K_{\mathrm{t}} \delta q \qquad (16)$$

up to the second-order terms; here p, q, f are column matrices, K_{t} a square matrix; T is the absolute temperature; $\delta^2 W$ is the second-order work of the reactions, i.e. the equilibrium load values (in the rare case that $\delta^2 W = 0$, the fourth variation needs to be analyzed similarly, which we do not discuss here). If the loads vary, the second-order work of loads must be added to the right-hand side of Equation (15). It can be shown that under isothermal conditions, $\delta^2 W = \delta^2 \mathscr{F} =$ second variation of Helmholtz free energy (or total energy) of the structure-load system under isothermal (or adiabatic) conditions. These energies represent the potential energies of the tangentially equivalent elastic structure expressed in terms of the isothermal (or isentropic) tangential moduli of the material.

The conceptual difference from elastic stability is that there are many potential energy expressions to consider, each of them valid in a different sector of the space of q, corresponding to different possible combinations of loading and unloading in various parts of the structure. The surfaces of second variation of entropy S (the negative of potential surfaces) in different sectors of this space are quadratic surfaces, which are joined continuously and with a continuous slope across the sector boundaries (Figure 7(b)). The eigenvector for a sectorial quadratic surface may lie inside or outside the corresponding sector. Only if it lies inside, the loss of positive definiteness of the potential surface (or negative definiteness of the entropy surface) in that sector is real and represents stability loss (e.g., in an elastoplastic column under gravity load, such a situation is first encountered when P reaches P_{r}, not P_{t}).

For the basic case of structures with a single load (or load parameter) P and the associated displacement q, the thermodynamic analysis shows that elastic as well as inelastic structures are stable as long as

$$\mathrm{d}P/\mathrm{d}q > 0 \qquad (17)$$

The stability limit is reached at the maximum (peak) load, and the postpeak states for which $\mathrm{d}P/\mathrm{d}q < 0$ are unstable. Under displacement control, the postpeak states are stable unless the softening slope (slope of the descending $P(q)$) curve becomes vertical; if the slope reverses from negative to positive, which is called the snapback, the structure becomes unstable (a stable response can nevertheless be obtained by controlling some internal displacements (e.g., the relative displacement across the damage band or crack)). A structure that exhibits postpeak softening ($\mathrm{d}P/\mathrm{d}q < 0$) will exhibit a snapback when it is loaded through a sufficiently soft spring. The snapback instability is reached when

$$\mathrm{d}P/\mathrm{d}q = -C \qquad (18)$$

where $C =$ stiffness of the loading spring. For elastic structures, postpeak softening can be caused only by buckling. Otherwise, it can also be caused by fracture or damage.

Thermodynamic analysis of bifurcation requires decomposing the infinitesimal loading step into two substeps. The first is a change away from equilibrium, in which the controlled loads or controlled displacements are changed without any change in the stress and deformation of the structure. The second substep is a restoration of equilibrium at constant controls. The equilibrium state approached in the

second substep may lie either on the primary (symmetry preserving) path or on the secondary (symmetry breaking) path, depending on which approach to equilibrium produces a larger entropy increment. In this manner one can prove in general, without considering imperfections, that the secondary path must occur. It is called the stable path. This is a different concept than that of stability of equilibrium (for inelastic structures, the post-bifurcation equilibrium states on both the primary and the secondary paths may be stable).

At small enough loads, the eigenvector for the quadratic entropy surface corresponding to the secondary path lies outside the sector of the displacement space in which this surface is valid. As the load increases, the eigenvector is turning, and at the first bifurcation load this sector first moves into the sector of validity of this surface. At that moment, the incremental equilibrium equations

$$K_t \delta q^{(1)} = \delta f \qquad (19)$$

and

$$K_t \delta q^{(2)} = \delta f \qquad (20)$$

for paths (1) and (2), respectively, must be valid simultaneously for the same load increment δf. So, by subtraction, one gets a homogeneous linear matrix equation for the difference of displacement increments:

$$K_t \left(\delta q^{(2)} - \delta q^{(1)} \right) = 0 \qquad (21)$$

Hence, the first bifurcation is indicated by singularity of the tangential-stiffness matrix K_t (Bažant and Cedolin, 1991), chap. 10; Hill, 1958; Maier *et al.*, 1973; Petryk, 1985; Nguyen, 1987). This matrix corresponds to loading (as opposed to unloading) at all points of the structures. Before the first bifurcation, the eigenvector of K_t is inadmissible because, in the displacement space, it lies outside the sector for which no point of the structure undergoes unloading. The orientation of this eigenvector rotates during loading and, at the first bifurcation, it lies at the boundary of this sector, thus making bifurcated path (2) admissible, for the first time during the loading process. After the first bifurcation, the eigenvector for the states on path (1) rotates inside this sector, and so a continuous series of bifurcation states lies on path (1).

The first bifurcation for a structure in which the tangential moduli are changing continuously can be determined by linear analysis of a solid without unloading (known as Hill's

(1962) linear comparison solid), in which the tangent modulus for loading applies everywhere. If the tangential moduli change by a jump, then the first bifurcation occurs when the smallest eigenvalue of K_t jumps from a positive to a negative value.

The use of the initial elastic stiffness matrix in load step iterations in FE programs may be deceptive. Convergence is lost if stability is lost, but not necessarily if the first bifurcation state on the primary loading path has been passed. Thus the iterations based on the initial elastic stiffness may, deceptively, converge for stable states lying on the primary path even if the first bifurcation state has been missed. Thus, if there is any danger of bifurcation, it is important to calculate the tangential stiffness matrix and check its positive definiteness. Imperfections in the sense of the eigenvector of K_t must be introduced to ensure that the bifurcation response be triggered in the computations (e.g., de Borst, 1987, 1989).

Phenomena such as friction or damage (or violation of the normality rule of plasticity) may cause the tangential stiffness matrix K to be nonsymmetric. If K is symmetric, positive definiteness is lost when det $K = 0$, which means that the stability loss under load control (gravity load) is characterized by neutral equilibrium. However, if K is nonsymmetric, the thermodynamic condition of stability limit (critical state), which reads

$$\delta q^T K \delta q = 0 \qquad (22)$$

can be satisfied not only when

$$\det K = 0 \qquad (23)$$

i.e., when there is neutral equilibrium,

$$K \delta q = 0 \qquad (24)$$

but also when the vector

$$K \delta q = \delta f \qquad (25)$$

is orthogonal to δf, i.e., when

$$\delta q^T \delta f = 0 \qquad (26)$$

This means that, for nonsymmetric $\hat{K}$, displacements with nonzero load increments may occur at zero work. Stability is decided by the symmetric part $\hat{K}$ of matrix K, whereas bifurcation or neutral equilibrium is decided by the singularity of the nonsymmetric matrix K.

According to the Bromwich theorem, the smallest eigenvalue of the symmetric $\hat{K}$ is less than or equal to the smallest real part of the eigenvalues of the nonsymmetric K. This

means that, in the case of friction or symmetry-breaking damage, positiveness of the real parts of the eigenvalues of the tangential stiffness matrix does not guarantee stability. Stability may be lost before the loading process leads to a bifurcation or a neutral equilibrium state,

$$\delta f = 0 \qquad (27)$$

at nonzero δq.

An inelastic structure may also be destabilized by load cycles. From the energetic viewpoint, stability in the standard sense (i.e., for one-way deviations from the equilibrium state) does not imply stability for infinitesimal deviation cycles and, vice versa, the latter does not imply the former. If infinitesimal strain cycles of a small material element increase entropy (i.e., produce negative second-order work), the material is locally unstable, which may (although need not) destabilize the structure. Drucker's (1951) postulate (equivalent to Hill's (1950) principle of maximum plastic work) prohibits such constitutive laws. This provides useful restrictions such as convexity of the yield surface and the normality rule for the strain rate vector in the 9D strain space. It also prevents the constitutive law from causing instabilities such as strain localization.

In the case of internal friction, however, the normality rule needs to be in some way relaxed. But then the flow rule, called nonassociated, typically produces localization instabilities (such as shear bands, cracking bands) which may or may not be real. It appears that the need for a nonassociated flow rule may often arise from adopting a single yield surface where in reality multiple yield surfaces intersecting at the current state point of the 9D strain space should be considered. The normal strain-rate vectors for all these surfaces may get superposed in a way that makes the resultant strain-rate vector appear not to be normal to the single yield surface defined by the yield limits for radial loadings. Such behavior is captured by the slip theory of plasticity of Taylor (1938) and Batdorf and Budiansky (1949), as well as by later generalization and modification in the form of the microplane constitutive model, which implies the existence of as many loading surfaces as there are mircoplanes (Bažant and Cedolin, 1991; Carol and Bažant, 1997).

By extensions of Mandel's (1964) stability analysis of an elastically restrained frictionally sliding block, it has been proved that, in frictional materials, a nonassociated flow rule does not cause instability if the strain-rate vector lies within a certain fan of directions. The fan is bounded by the normal to the yield surface and the normal to the surface of the so-called frictionally-blocked second-order elastic energy density. Simple formulations are available for two cases: (i) direct internal friction, representing the effect of hydrostatic pressure on deviatoric yielding; and (ii) so-called inverse friction, representing the effect of stress invariant J_2 on the inelastic volume change (Bažant and Cedolin, 1991, section 10.7).

2.02.3.5 Stability Problems of Fracture Mechanics

Plasticity and hardening damage of the material profoundly affects the stability of structures but this does not cause instability. The cause lies solely in the nonlinear geometric effect of deformations. Alternatively, fracture and softening damage (such as microcracking or plastic micro-void growth) can destabilize a structure, even in absence of the nonlinear geometric effect.

The energy balance condition of crack propagation is $g = R(c)$, where $g =$ energy release rate, and $R(c) = R$-curve = critical value of g depending in general on the crack extension c. This condition plays the role of an equilibrium condition—the crack can grow statically. For $g > R(c)$ the growth is dynamic, and for $g < R(c)$ no growth is possible. Under load control, the limit of stability of a structure with a statically growing crack is reached at maximum load, which occurs when
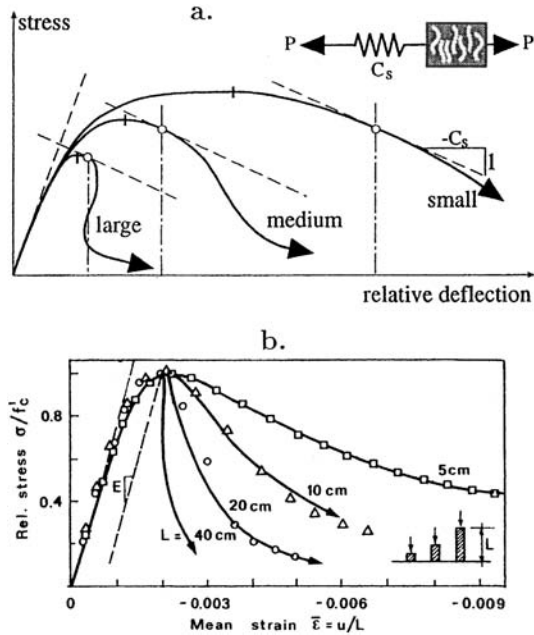
$$[\partial g / \partial c]_{\mathrm{P}} = \partial R(c) / \partial c \qquad (28)$$

Replacing $=$ with $>$ yields the stability condition. The stability limit for loading through a spring, which characterizes the ductility of a structure, can be determined by calculating the load-deflection curve, which can be done on the basis of a solution of the stress intensity factor. Under displacement control, fracture growth becomes unstable when the postpeak descending load-deflection curve reaches a snapback (Figure 9(a)). Some structure geometries never exhibit a snapback instability (unless loaded through a soft enough spring), while others do. The former is the case, e.g., for notched three-point bend beams. The latter is the case whenever the ligament is subjected to a normal force (which is called ligament tearing, occurring, e.g., in notched tensile strip specimens).

The R-curve is the simplest (and crudest) way to take into account the finiteness of the fracture process zone at the crack tip. This property, which is more accurately described by the cohesive crack model or the crack band model, gives rise to a deterministic size effect on the nominal strength of geometrically

similar structures with geometrically similar failure modes. By measuring the size effect in notched specimens, one can deduce the *R*-curve and the main parameters of the cohesive crack model.

Simultaneous growth of many cracks (of length a_i, $1 = 1, 2, \ldots$) typically produces bifurcation as well as stability loss (Figures 10 and 11(a)). The incremental potential $\delta^2 F$ (equal to the negative of the second-order entropy, or free energy) is characterized by a matrix that involves the partial derivatives $\partial K_i / \partial a_j$ where K_i is the stress intensity factor of crack i. The potential surface is a patch-up of many quadratic sectors joined continuously and smoothly (Figures 11(b) and (d)). In multicrack systems, the advance of one crack tip often causes unloading of the nearby crack tip, with the result that only one of the cracks can grow. This for instance happens for symmetrically edge-cracked and center-cracked tensioned strip specimens, in which there are two interacting crack tips.

Another example is the system of parallel equidistant cracks in an elastic halfplane, driven by cooling or drying shrinkage (Figure 10(a); Bažant and Cedolin, 1991, section 11.2). As the cooling front advances into the halfplane, the cracks first grow while keeping equal length (primary path). At a certain moment (Point A in Figure 10(b)), a stable bifurcation of the equilibrium path is reached. For the bifurcated (secondary) path, which is the stable path (i.e., must occur), every other crack stops growing (Figure 10(a)) and gradually closes, while the growing cracks gradually open wider. If the cracks are somehow kept equally long after the bifurcation, a stability limit (B in Figure 10(b)) is eventually reached. The behavior is analogous to elastoplastic columns. The parallel crack system, however, may be stable, with no crack arrest, if the cooling temperature profile is rather flat and has a sufficiently steep front, or if the halfplane is reinforced by bars near the surface.

Similar bifurcations and instabilities are exhibited by parallel cracks in the tensile zone of beams subjected to bending. Such bifurca-
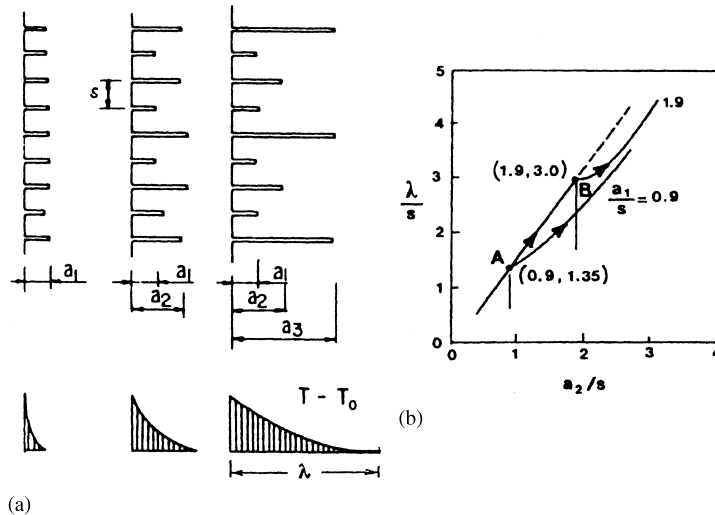

Figure 9 (a) Typical diagrams of nominal stress versus relative deflection for structures of different sizes, exhibiting strain-softening damage of fracture (with stability limits for loading device of stiffness C_s). (b) Effect of localization in compressed concrete prisms of various lengths calculated by crack band model, and test data of van Mier (1986).

Figure 10 Evolution of a system of parallel cooling cracks and depth of cooling penetration λ versus length a_2 of leading cracks.
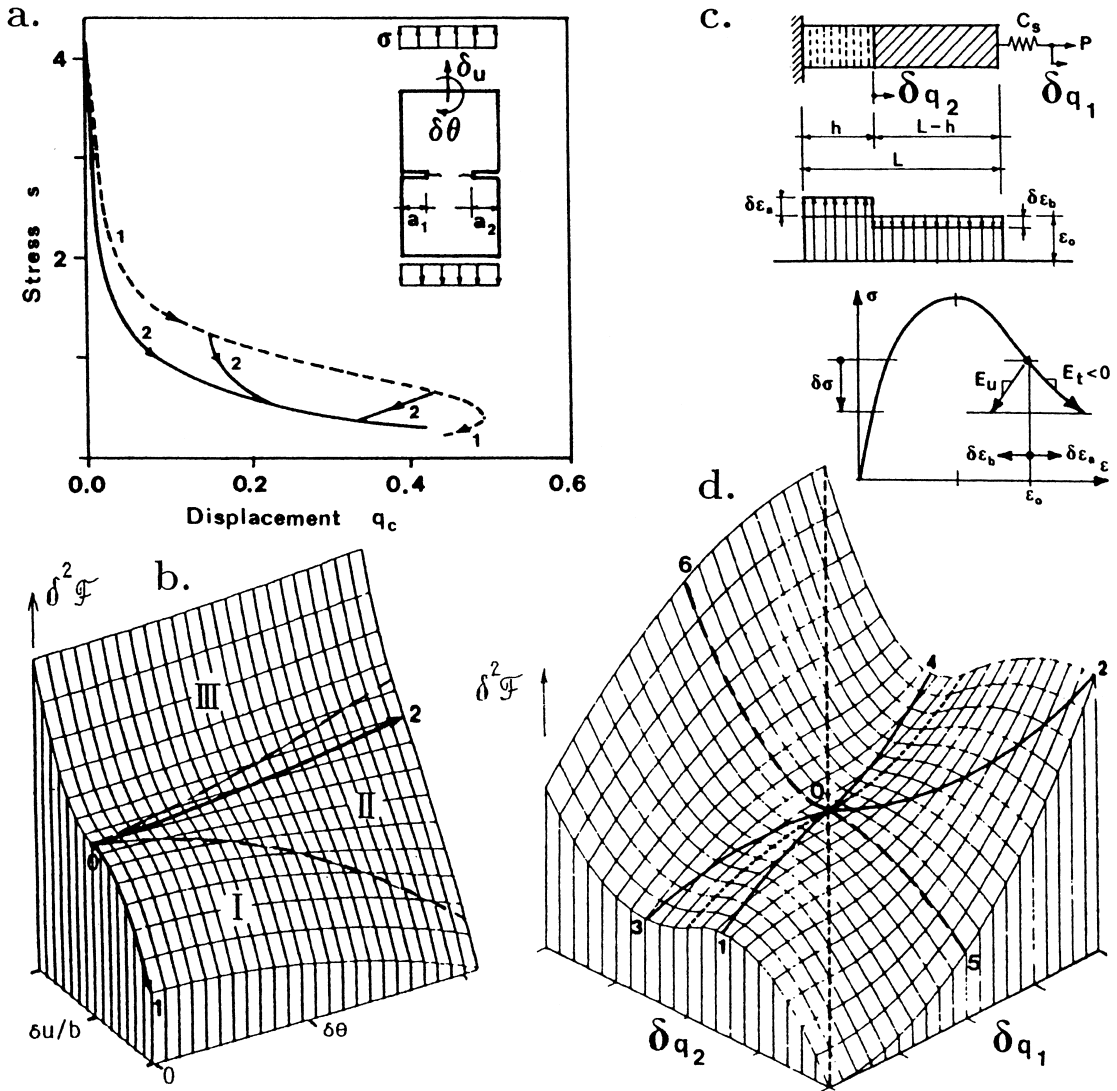
Figure 11 (a) Double-edge cracked specimen—diagram of average stress versus displacement, with bifurcations (solid curve: one crack growing; dashed: both growing). (c) Longitudinal localization of strain softening in a tensioned bar. (b and d) Corresponding surfaces of incremental potential $\delta^2 F$ (= minus second-order entropy increment) showing bifurcations and instabilities (02 or 05) under controlled axial displacement.

tions determine the spacing of deep cracks and ductility of the structure. The initial crack spacing can be determined (Li *et al.*, 1995) by considering a sudden formation of cracks of length a_0 and stipulating three conditions: (i) the material tensile strength is reached before the cracks appear, (ii) the energy released from the structure caused by a finite crack jump of length a_0 is equal to the total energy dissipated by the creation of the initial cracks of length a_0, and (iii) the energy release rate for further growth of cracks of length a_0 is critical. The bifurcations in a system of parallel cracks are important because they decide the width of cracks, which controls the overall effective permeability and the rate of ingress of corrosive agents into structures.

In 3D, an approximate analysis of the entropy increment confirms that a hexagonal pattern of cooling or drying cracks on a halfspace surface (as seen, e.g., on a drying lake bed or a cooling lava flow) should be favored over triangular and square patterns as well as parallel planar cracks. However, accurate solutions of the bifurcation and stability of 3D cracks seem unavailable.

2.02.3.6 Damage Localization Instabilities and Size Effect

Continuum damage mechanics provides a smeared description of the growth of microcracks in brittle materials or voids in plastic

materials. Of main interest is the damage that causes strain softening—a phenomenon manifested by a negative slope of the stress–strain curve and generally by a loss of positive definiteness of the matrix of tangential moduli. Such a material behavior violates Drucker's postulate (or postulates of maximum plastic work, Jirásek and Bažant, 2002) and leads to localization instabilities and bifurcations, and to size effect (Bažant and Chen, 1997; Bažant, 1999). Formation of softening hinges in beams and frames also causes bifurcations (Maier *et al.*, 1973) and, inevitably, localization instabilities and size effect (Bažant, 1986, 2001, 2002a, 2002b; Jirásek and Bažant, 2002; Bažant and Jirásek, 2002), in not only static but also in dynamic (seismic) loading (Bažant and Jirásek, 1996), and so does softening in friction (particularly the frictional stress drop from static friction to dynamic friction); see also Rice and Ruina (1982).

Although strain-softening stress–strain relations have been used in concrete engineering since the 1950s and in FE analysis since 1968 (Bažant, 1986), until about 1985 most mechanicians regarded all strain-softening studies with contempt (research into this "dubious" concept was even banned in some communist countries), although, curiously, the continuum damage mechanics, which exhibits (without regularization based on some characteristic length) the same localization instabilities as any strain softening model, nevertheless escaped condemnation, perhaps because the strain softening was disguised as a separate damage variable while the "true" stress exhibited only hardening (a regrettable consequence has been that efforts to regularize continuum damage mechanics formulations have been lagging).

Today, however, the strain-softening damage is a well-established and indispensable concept—but of course only within the context of some nonlocal material model possessing a characteristic length.

In absence of a characteristic length, one objectionable property of strain softening is that if the elastic moduli matrix ceases being positive definite, the material cannot propagate waves and the dynamic initial-boundary value problem changes its type from hyperbolic to elliptic (Hadamard, 1903). Since the unloading modulus is always positive (as experimentally discovered for concrete in the 1960s), the material can nevertheless propagate unloading waves. A strain-softening material can also propagate loading waves of a sufficiently steep wave front (Bažant and Li, 1997) because, as transpired from experiments (Bažant *et al.*, 1995), a sudden increase of the loading rate temporarily reverses strain softening to strain hardening (which explains why ultrasound can pass through strain-softening concrete specimens).

That the concept of strain-softening is not mathematically meaningless was demonstrated by analyzing converging step waves produced in a rod when the ends are suddenly forced to move inward at constant velocity. After the waves meet, two kinds of responses can occur: (i) if the strain front magnitude is less than one half of the strength limit (onset of strain softening), the waves get superimposed and the stress front doubles; but otherwise (ii) the stress drops instantly to zero, the bar splits, and unloading waves emanate from the split. The dynamic problem is ill-posed (and the solution is unstable) because an infinitely small change in the velocity imposed at the ends of the rod can cause a finite change in the response. The solution nevertheless exists. But there is a problem: the splitting of the bar occurs with zero energy dissipation, which makes a strain-softening concept with no characteristic length physically unacceptable (Bažant and Cedolin, 1991). Similar unstable and physically unrealistic solutions have been mathematically demonstrated for waves in a rod in which the strain softening is followed by rehardening, and also for radially converging waves in a strain-softening sphere.

Rudnicki and Rice (1975) and Rice (1975, 1976) pioneered analysis of static localization of plastic (nonsoftening) strain into a planar band (e.g., a shear band) in an infinite body. Such localization is caused by the nonlinear geometric effect of finite strain and occurs very near the yield stress value. If strain softening takes place, its destabilizing effect is normally much stronger than that of geometric nonlinearity. Bifurcation of the localization type is decided merely by the constitutive law; it occurs when the so-called acoustic tensor

$$\boldsymbol{A} = \boldsymbol{n} \cdot \boldsymbol{C}^t \cdot \boldsymbol{n} \tag{29}$$

becomes singular (where $\boldsymbol{C}^t =$ fourth-order tangential moduli tensor, and $\boldsymbol{n} =$ unit normal of the localization band). Various damage constitutive laws have been analyzed with regard to the singularity of $\boldsymbol{A}$.

Localization can also be triggered by a lack of normality of plastic flow (de Borst, 1988; Leroy and Ortiz, 1989). In the case of infinite space, this condition represents the stability limit as well. But for an infinite planar localization band of finite thickness h located within an infinite layer of finite thickness $L > h$, the stability limit occurs later and is character-

ized by singularity of the tensor

$$\boldsymbol{Z} = \boldsymbol{n} \cdot [\boldsymbol{C}^t + \boldsymbol{C}^u h/(L-h)] \cdot \boldsymbol{n} \qquad (30)$$

where $\boldsymbol{C}^u$ = material stiffness tensor for unloading. For $L/h \to \infty$, the condition for the acoustic tensor is recovered.

When a localization band much longer than its thickness cannot develop, because of a finite size of the body, a more realistic, yet analytically solvable, model is the localization of softening damage into an ellipsoidal region. This has been solved with the help of the Eshelby theorem giving the strain of an ellipsoidal plug that has been fitted into a different ellipsoidal hole in an infinite elastic body (Bažant and Cedolin, 1991, section 13.4). The bifurcations and instabilities are found to depend on the aspect ratios of the ellipsoid and occur later in the loading process than for an infinite band.

The usefulness of the bifurcation studies of constitutive laws, however, is rather limited—they reveal only the onset of localization, while often it is much more important to determine the postbifurcation behavior of a body containing a damage localization region. In this regard, the concept of strain softening (or continuum damage) requires a characteristic length (or material length) in order to overcome certain fundamental difficulties.

In a strain-softening bar, a uniform axial strain cannot occur. The strain inevitably localizes into a band (or fracture process zone) of the smallest possible length. Consequently, the longer the bar, the steeper is the postpeak curve of stress vs. average strain (Figure 11(c)). A nonlocalized strain distribution loses stability when the softening load-deflection slope reaches a certain magnitude (Figure 11(a)) depending on the structure size and the stiffness of the loading device (the stability limit is the only objective and sound approach to defining the ductility of a structure; Bažant, 1976).

An analytical solution of a tensioned bar subdivided into FEs exhibits bifurcations. Their consequence is that the strain softening must usually localize into a single FE, no matter how small the element may be. Numerical FE computations of strain-softening damage under static loading may converge, but to a wrong solution. They reveal spurious mesh sensitivity—the postpeak load-deflection curves of structures with strain softening are unobjective because very different peak loads and postpeak responses are obtained for different element sizes. The energy dissipated by breaking the structure converges to zero as the FE size is reduced to zero. These are physically unrealistic features. The remedy consists in introducing some form of a nonlocal continuum model possessing a characteristic length (Bažant and Jirásek, 2002; Jirásek and Bažant, 2002), of which there are basically three types:

(i) the crack band model,
(ii) the integral-type nonlocal model, and
(iii) the second-gradient model;

(the first-gradient or Cosserat-type models did not turn out to be effective for localization of tensile damage). The first and third type can be regarded as approximations to the second.

The crack band model (Bažant, 1976, 1982; Bažant and Oh, 1983; Bažant and Cedolin, 1991, ch. 13; Bažant and Planas, 1998), is the crudest but simplest (and thus preferred in concrete design firms and commercial programs). Its salient characteristic is to impose a certain characteristic size h of the FE, which must be regarded as a material property, representing a characteristic length l of the material; l corresponds to the width of the crack band (or strain-softening damage band). In the case that localization of strain-softening damage is not prevented by some restraints such as reinforcing bars, the crack band model is essentially equivalent to the cohesive (or fictitious) crack model, in which the crack opening is equal to the cracking strain accumulated over the width of the crack band. Various semi-empirical energy-based numerical corrections need to be used when the band does not propagate along the mesh lines (Červenka and Červenka, 1998).

In the nonlocal continuum concept, which was introduced for elasticity by Eringen (1965), the stress at a given point depends not only on the strain at that point but also on a certain average of the strain field in a neighborhood of the point, whose effective size corresponds to the characteristic length l of the continuum. The average is weighted by a bell-shaped weight function. When the nonlocal concept was introduced in 1984 for the purpose of limiting the localization of strain softening, the total strain was averaged over the neighborhood. However, this caused two problems: the numerical implementation was cumbersome (requiring imbrication of FEs), and zero-energy periodic modes of instability developed and had to be suppressed by an artificial parallel overlay.

The problems of the total strain averaging were overcome in 1987 by the nonlocal damage model, in which the spatial averaging is done on the damage variable or the inelastic part of strain. With this concept, localization of strain to form a displacement discontinuity line is impossible (the reason for this is that if the

strain profile became a function with C_0 continuity (Dirac delta function), the averaging integral would convert the profile in the next iteration to a function with C_1 continuity (Heaviside step function)). The nonlocality of damage can be physically justified (Bažant and Jirásek, 2002) by the smoothing of an array of discrete cracks and by crack interactions (the latter, however, also points to a more complicated nonlocal model which distinguishes the directions of amplifying and shielding crack interactions; Bažant, 1994; Bažant and Planas, 1998). FE studies demonstrate that the nonlocal damage model is free of zero-energy periodic modes of instability, eliminates spurious sensitivity, effectively limits excessive damage localization, and correctly simulates the size effect on the nominal strength as well postpeak behavior. However, studies (Jirásek, 1998b) revealed that the nonlocal processing of inelastic strain does not suffice for simulating complete fracture with a zero stress across the softening band. Rather, an "over-nonlocal" inelastic strain, proposed simultaneously and independently in 1996 by Planas and colleagues (cf. Bažant and Planas, 1998) and by Strömberg and Ristinmaa (1996) is needed for that.

The nonlocal concept makes sense only if the FEs are at least three-times smaller than the characteristic length *l*, and this is also required to make the propagation direction of a damage band independent of the mesh layout. If the number of elements of this size would be excessive, one may use the crack band model, for which the FE size should optimally be *l* but can be much larger. If the number remains excessive, one may use a variant of the crack band or cohesive crack model, the idea of which is to embed in the FE either a crack band (a strain-softening strip limited by strain discontinuity lines) or a cohesive crack (a line of displacement discontinuity), (Ortiz *et al.*, 1987, Belytschko *et al.*, 1988). There are two basic simple forms of such models—kinematically consistent and statically consistent. But it is their combination that is found to be optimal (Jirásek, 1998a, 1998b). The embedded discontinuity models are best to model the final stage of damage in which the distributed cracking coalesces into a distinct fracture. But there is a mesh bias for the propagation direction—when the mesh lines are not laid in the correct direction of fracture propagation, the correct orientation of the crack band or discontinuity is not obtained, and the error in orientation can be very large. As shown by Jirásek (1998a), it is best to use the nonlocal model at the beginning, in order to capture the correct discontinuity orientation, and later switch to an embedded discontinuity model.

In the nonlocal damage model, the need to calculate averages over a group of FEs increases the bandwidth, and the use of asymmetric averaging near the boundaries makes the stiffness matrix nonsymmetric. Although the asymmetry resulting from nonlocality causes does not destabilize computational simulations, it is inconvenient for some types of numerical algorithm. This drawback can be avoided by second-gradient damage model—a weakly nonlocal model in which the nonlocal variable is obtained from a linear combination of the local variable and its Laplacian, as proposed in 1984 (Bažant and Cedolin, 1991, Equation 13.10.25) for a model derived (and physically justified) by Taylor series expansion of the weight kernel in the nonlocal averaging integral and by truncation after the quadratic term. The truncation, however, is physically questionable because crack interactions, from which a nonlocal model can be derived (Bažant, 1994), have a rather slow decay with distance.

A drawback of the second-gradient approximation of the nonlocal model is the C_1 continuity required for the strain field in the FE. This drawback can be circumvented by a strongly nonlocal formulation of Peerlings *et al.* (1996) obtained by expressing the local variable as a linear combination of the nonlocal variable and its Laplacian. As discovered by Peerlings *et al.* (1996), this drawback can be circumvented by inverting the nonlocal operator—the nonlocal variable is expressed as a linear combination of the nonlocal variable and its Laplacian, which provides an additional separate partial differential equation (Helmholtz equation) from which the nonlocal variable is solved. De Borst and co-workers have shown that this approach yields very good results.

The main practical consequence of the damage localization instabilities and of the existence of a characteristic length of the continuum is the size effect, both on the nominal strength of structures and on the postpeak response. Numerical studies of nonlocal and gradient models of geometrically similar structures of different sizes, exhibiting similar damage band paths, show that the maximum loads approximately follow the simple size effect law proposed in 1984 by Bažant (e.g., Bažant and Cedolin, 1991, chaps. 12 and 13; Bažant and Planas, 1998; Bažant and Chen, 1997). This law has been amply verified experimentally, and has been derived (Bažant 1997, 1999, 2002a; Bažant and Chen, 1997; Bažant *et al.* 1999) from fracture mechanics and limiting plastic solutions by applying the technique of asymptotic matching.

The size effect has been shown important for the design of large concrete structures, for assessments of failure and seismic response of large bodies in geotechnical engineering and geophysics, for Arctic ice studies, etc. The size effect law provides an important check on the validity of a numerical model, and the size effect measurements can be exploited to calibrate the main model parameters. Large size effects due to damage localization and stable growth of large fractures are observed not only in concrete (and mortar)—the problem so far studied most, but also in tensile and compression failures of fiber-polymer composites (Bažant *et al.*, 1999), sea ice (Bažant and Kim, 1998), rocks and ceramics (Bažant and Planas, 1998), wood, and probably in all the other quasibrittle material including toughened ceramics, polymer and asphalt concretes, particulate composites, wood particle board, bone, biological shells, stiff clays, cemented sands, grouted soils, coal, paper, various refractories, some special tough alloys, rigid foams and filled elastomers (Bažant, 2002a).

2.02.4 NONLINEAR 3D FINITE-STRAIN EFFECTS ON STABILITY

2.02.4.1 Finite-strain Effects in Bulky or Massive Bodies

To determine the critical state, the potential energy must be expressed accurately up to the quadratic terms. For the strain energy, this condition is satisfied if the small (linearized) strain expressions are used. But the potential energy also includes the work of the initial stresses S_{ij} which are finite. Therefore, the strains on which S_{ij} work must be expressed accurately up to their second-order terms (the subscripts label the Cartesian coordinates $x_i, i = 1, 2, 3$). Therefore, a finite strain expression that is correct up to the second-order terms in the displacement gradient must be used.

Any tensor $\boldsymbol{\varepsilon}$ satisfying the following three conditions can be used as a measure of finite strain: (i) $\boldsymbol{\varepsilon}$ must vanish for all rigid-body motions; (ii) $\boldsymbol{\varepsilon}$ must be a symmetric tensor (because the stress tensor, which is symmetric, would do zero work on an antisymmetric part); and (iii) $\boldsymbol{\varepsilon}$ must be continuous and continuously differentiable, and its matrix must be invertible (Bažant and Cedolin, 1991; Rice 1993). For convenience, a fourth condition is imposed; $\boldsymbol{\varepsilon}$ must, for small deformations, reduce to the standard small-strain tensor. There are many finite strain tensors satisfying these conditions (Bažant and Cedolin, 1991; Rice, 1993; Ogden, 1984). A very general class of finite strain

tensors consists of the Doyle–Ericksen (1956) strain tensors,

$$\boldsymbol{\varepsilon} = \frac{1}{m}(\boldsymbol{U}^m - 1) \quad \text{for } m \neq 0, \qquad \boldsymbol{\varepsilon} = \ln \boldsymbol{U} \quad \text{for } m = 0 \tag{31}$$

where $\boldsymbol{U} =$ right-stretch tensor and m is an arbitrary real number. These tensors have the second order approximation:

$$\varepsilon_{ij}^{(m)} = \varepsilon_{ij} - \tfrac{1}{2}m\, e_{ik}e_{kj} \tag{32}$$

where e_{ik} is the small (linearized) strain tensor, $m = 2$ gives Green's Lagrangian strain tensor, while $m = 1$ and $m \to 0$ provide the second-order approximations to Biot's (1965) strain tensor and to Hencky's (logarithmic) strain tensor, respectively.

For beams, plates and shells with negligible transverse shear deformations, the choice of m makes no difference because the second-order work of the initial axial or in-plane stresses depends only on the rotations of the cross sections or the normals. However, for massive bodies, and for slender beams or shells soft in shear (such as sandwich structures), the choice of m does make a difference.

Historically, beginning with Southwell (1914) and Biezeno and Hencky (1928), various stability formulations associated by work with $m = 2, 1, 0, -1, -2$ have been proposed. The differential equations of equilibrium for deviations from the initial state, the quadratic variational principles and the critical load solutions for these formulations seemed to differ and be in conflict. This generated unnecessary long-running polemics and controversies (see, e.g., the preface of Biot's (1965) book, or various comments in works of Truesdell). As it turned out, however, all these formulations are equivalent (Bažant, 1971a; Bažant and Cedolin, 1991, chapter 11) because the tangential moduli tensors $C_{ijkl}^{(m)}$ for different m and the same material are not the same; according to the requirement of equality of second variation of work, they are related as

$$C_{ijkl}^{(m)} = C_{ijkl} + \frac{(2-m)}{4}$$
$$\times (S_{ik}\delta_{jm} + S_{jk}\delta_{im} + S_{im}\delta_{jk} + S_{im}\delta_{ik}) \tag{33}$$

(Bažant, 1971a; Bažant and Cedolin, 1991, section 11.4) where C_{ijkl} are the tangential moduli associated with Green's Lagrangian strain tensor ($m = 2$), and δ_{ij} is Kronecker's delta (note that in the literature there also exist formulations in which the objective stress increments do not correspond to the same m as the moduli C_{ijkl}, but this is incorrect). Obviously, the differences among the $C_{ijkm}^{(m)}$
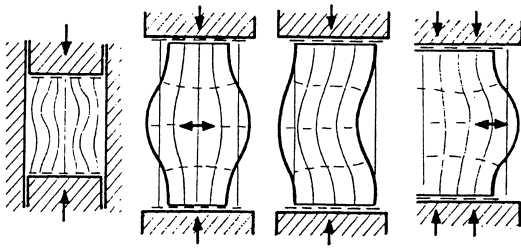
Figure 12 Basic types of 3D buckling.

values for different m are insignificant if the (suitable) norms

$$\left\| S_{ij}(\boldsymbol{x}) \right\| \ll \left\| C_{ijkm}^{(m)}(\boldsymbol{x}) \right\| \quad \text{(for every } \boldsymbol{x}) \quad (34)$$

where $\boldsymbol{x}$ are coordinate vectors of points in the structure.

The 3D buckling instabilities and the differences in tangential moduli corresponding to different choices of the finite strain tensor are important if and only if some of the principal values of the tangential elastic moduli tensor is of the same order of magnitude as the initial stresses at the same point or, in the case of slender structures, at the same cross section. This can for instance occur for materials that undergo a drastic reduction of tangential stiffness due to plasticity or damage and develop shear bands, cracking bands or crushing bands. Simple analytical solutions have been obtained for a number of important problems, e.g., periodic internal buckling of a compressed massive orthotropic body, periodic surface buckling of a compressed othotropic halfspace or layered halfspace (folding of strata, in geology), and bulging or buckling of a compressed thick orthotropic rectangular specimen (Figure 12; see Biot (1965) and a generalization in Bažant (1971a) and in Bažant and Cedolin, 1991, chap. 11).

2.02.4.2 Nonlinear Finite-strain Effects in Columns, Plates and Shells Soft in Shear

Another important class of stability problems where the differences in tangential moduli corresponding to different choices of the finite strain tensor are important consists of columns, plates and shells soft in shear. This important class includes:

(i) highly anisotropic materials such as composites with a soft (polymeric) matrix, reinforced by stiff (carbon, glass) fibers in only one or two directions;

(ii) composite slender structures with a core soft in shear, such as sandwich columns, plates and shells;

(iii) continuum approximations of built-up columns, either battened columns or lattice columns, the cells of which are normally soft in shear;

(iv) continuum approximations to layered elastomeric bearings of the type used for bridges and for seismic isolation of buildings; and

(v) helical springs, the shear stiffness of which is typically quite low.

There has been a long-lasting (but unnecessary) controversy between two different formulas for critical stress, one derived by Engesser (1889), with applications for built-up columns in mind, and another derived by Haringx (1942) for helical springs;

$$P_{\mathrm{cr}} = \frac{P_{\mathrm{E}}}{1 + (P_{\mathrm{E}}/GA)} \quad \text{(Engesser)} \quad (35)$$

$$P_{\mathrm{cr}} = \frac{GA}{2}\left(\sqrt{1 + \frac{4P_{\mathrm{E}}}{GA}} - 1 \right) \quad \text{(Haringx)} \quad (36)$$

(see also Timoshenko and Gere, 1961); E, G are elastic Young's and shear moduli respectively, $P_{\mathrm{E}} = \left(\pi^2/l^2 \right) EI =$ Euler's critical load (for a column without shear deformations), l is the effective buckling length, and EI, GA are bending stiffness and shear stiffness of the cross-section, respectively (note that, in general, $A = \kappa A_0$ where $A_0 =$ actual cross-section area and $\kappa =$ Timoshenko's shear correction factor, which is greater than, but close to, 1; for a sandwich $\kappa \approx 1$). Each of these two formulae can be regarded as a different and equally plausible generalization of the Timoshenko beam theory (Timoshenko, 1921), which does not deal with finite-strain effects and applies only to beams carrying negligible axial force.

The discrepancy between these two formulae used to be, before 1971, regarded as a controversial paradox. Then it was shown (Bažant, 1971a; Bažant and Cedolin, 1991, chap. 11) that this classical paradox is caused by a dependence of the tangential shear modulus $C_{1212} = G$ on the axial stress $S_{11} = -P/A$, which inevitably is different for different choices of the finite-strain measure, i.e., for different m. It turns out that Engesser's formula corresponds to Green's Lagrangian strain tensor ($m = 2$), and Haringx's formula to the Lagrangian Almansi strain tensor ($m = -2$). Therefore, the shear moduli in Engesser's and Haringx's formulas (35) and (36) should have different notations; we denote them from now on as $G^{(2)}$ and $G^{(-2)}$, respectively. From (33), it follows that

$$G^{(2)} = G^{(-2)} + P/A \quad (37)$$

The difference in the E-values indicated by (33) for $m = 2$ and $m = -2$ can be neglected because the axial stress is always negligible compared to the E value for the skins.

Replacing G in Engesser's formula with $G + P_{cr}/A$ and solving P_{cr} from the resulting equation (Bažant and Cedolin, 1991, p. 738), one obtains Haringx's formula, which makes the equivalence blatant and resolves the old paradox. The difference in shear moduli in (37) is important only if the axial stress $S_{11} = -P/A$ is not negligible compared to G. Equation (37) makes it also clear that if the shear modulus is constant (independent of stress $-P/A$) for one formula, it cannot be considered constant for the other formula.

2.02.4.3 Discrepancy between Engesser's and Haringx's Formulas: New Paradox and its Resolution

Though a new kind of paradox has arisen from some experimental studies and 3D FE simulations of sandwich columns (Kardomateas, *et al.*, 2002; cf. Bažant, 2002b). Let l be the length of a pin-ended sandwich column; h the thickness and G the elastic shear modulus of the core. The skins have thickness t and axial elastic modulus E (Figure 13, left). Young's modulus of the core is negligible, but since $t \ll h$ the entire shear force is carried by the core. Therefore, one may substitute

$$EI = R = Ebt(h + t)^2/2 + Ebt^3/6 \approx Ebth^2/2 \quad (38)$$

which represents the bending stiffness of the sandwich $(t \ll h)$, and

$$GA = H = Gbh \quad (39)$$

which represents the shear stiffness of the sandwich, b being the cross-section width. With these substitutions, the Engesser and Haringx formulas become

$$P_{cr} = \frac{P_E}{1 + (P_E/Gbh)} \quad \text{(Engesser type)} \quad (40)$$

$$P_{cr} = \frac{Gbh}{2}\left[\sqrt{1 + \frac{4P_E}{Gbh}} - 1\right] \quad \text{(Haringx type)} \quad (41)$$

where P_E is the Euler load,

$$P_E = \frac{\pi^2}{l^2}EI \approx \frac{\pi^2}{l^2}\frac{Ebth^2}{2} \quad (42)$$

Similar to (37), one may check that, by making the replacement

$$G_{core} \leftarrow G_{core} - \frac{2t}{h}\sigma_{skins} \quad (43)$$

where $\sigma_{skins} = -P_{cr}/2bt$ and $G = G_{core} = $ shear modulus of the core, the Engesser-type formula (40) gets transformed into the Haringx-type formula (41).

Although the foregoing replacement works, it is, however, purely formalistic, with no physical basis. It is certainly paradoxical that the shear modulus in the *core* should depend on the axial stress in the *skins*. Therefore, the reason for the discrepancy between these two formulas cannot be caused by the differences in the shear modulus G of the core material, as given by Equation (37). Besides, there is no reason for the G-moduli associated with diverse strain measures to differ because the axial stress in the core of sandwich columns is always negligible compared to the shear modulus of core.
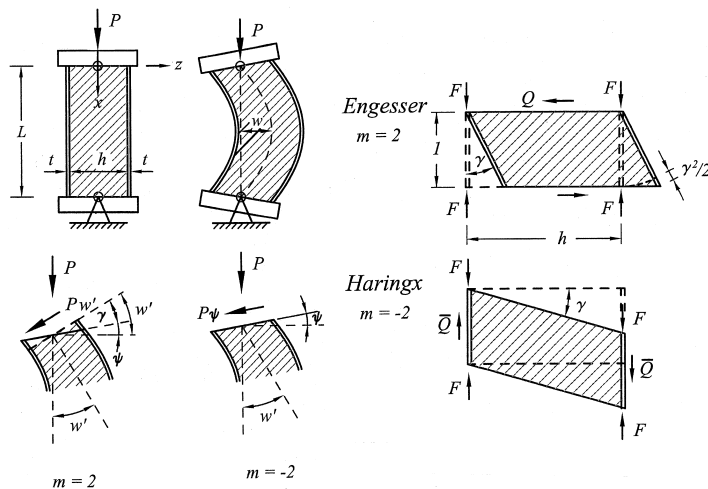
Figure 13 Top left: buckling of hinged sandwich column. Bottom left: rotation angles and internal forces in sandwich column. Right: second-order shortening due to shear deformations.

Realizing these points created a new kind of paradox and generated polemics at recent conferences. To explain it, Bažant (2002b) noticed that one must not limit consideration to the material level, as in Equation (43). Rather, one must consider from the outset a sandwich column constrained by the hypothesis that (in slender enough columns) the cross sections of the core must remain plane. It may be shown (Bažant, 2002b) that the second variation of the potential energy Π of a sandwich column expressed on the basis of Doyle–Ericksen finite-strain tensors with arbitrary m can be expressed as

$$\delta^2 \Pi = \frac{1}{2} \int_0^L \left\{ R^{(m)} \psi'^2 \right.$$
$$\left. + \left[H^{(m)} + \frac{1}{4}(2-m)P \right](w' - \psi)^2 - Pw'^2 \right\} dx$$
$$(44)$$

where $w = w(x) =$ lateral deflection as a function of axial coordinate x, $H^{(m)}$ and $R^{(m)}$ are the shear and bending stiffness associated with m, and the primes denote derivatives with respect to x. Proceeding in the standard way (Bažant and Cedolin, 1991) according to the calculus of variations, one obtains for $m = 2$ and $m = -2$ the linear differential equation

$$w'' + k^2 w = 0 \qquad (45)$$

for column deflections $w(x)$, and the boundary conditions $w = 0$ at $x = 0$ or l. The expressions for parameter k^2 as a function of load P are different for different m, and this leads to two different critical load formulas analogous to those of Engesser and Haringx:

for $m = 2$:

$$P_{\mathrm{cr}} = \frac{P_{\mathrm{E}}^{(2)}}{1 + \left(P_{\mathrm{E}}^{(2)} / H^{(2)} \right)}$$
$$\text{with} \quad P_{\mathrm{E}}^{(2)} = \frac{\pi^2}{l^2} R^{(2)} \qquad (46)$$

for $m = -2$:

$$P_{\mathrm{cr}} = \frac{H^{(-2)}}{2} \left[\sqrt{1 + \frac{4 P_{\mathrm{E}}^{(1-2)}}{H^{(-2)}}} - 1 \right]$$
$$\text{with} \quad P_{\mathrm{E}}^{(-2)} = \frac{\pi^2}{L^2} R^{(-2)} \qquad (47)$$

It has been shown (Bažant, 1971a; Bažant and Cedolin, 1991) that the case $m = 2$ is associated by work with Truesdell's (1955) (objective) stress rate, and the case $m = -2$ with Cotter and Rivlin (1955) convected (objective) stress rate or with Lie derivatives

of Kirchhoff stress. Using other m values, one could further obtain from Equation (44) an infinite number of sandwich buckling formulas. Curiously, however, no investigators proposed critical load formulas associated with m other than 2 and –2, although many investigators (e.g., Biot, 1985; Biezeno and Hencky, 1928; Neuber, 1965; Jaumann, 1911; Southwell, 1914; Oldroyd, 1950; Truesdell, 1955; Cotter and Rivlin, 1955—see Bažant and Cedolin, 1991, chap. 11) introduced formulations for objective stress rates, 3D stability criteria, surface buckling, internal buckling, and incremental differential equations of equilibrium associated with $m = 1$, 0, and –1.

In analogy to Equation (37) and similarity to Equation (43), one may expect the shear stiffnesses for the Engesser's and Haringx's formulas to be related as

$$H^{(2)} = H^{(-2)} + Ph/2t \qquad (48)$$

Indeed, when this relation is substituted into Engesser's formula (46) and the resulting equation is solved for $P = P_{\mathrm{cr}}$, Haringx's formula (47) ensues. However, unlike homogeneous columns soft in shear, the foregoing transformation cannot be physically justified in the sense of Equation (43), i.e., on the basis of the general transformation of tangential moduli in Equation (33) nor its special case in Equation (37). The reason is that the axial stress S^0 in the core is much smaller than the axial elastic modulus E for the core, and in fact negligible.

From this viewpoint, the transformation in Equation (43) appears illogical: why should the shear modulus of the core be adjusted according to the axial stress in the skins? This has become a new apparent paradox. To resolve it, we need to take a closer look at the definition of the shear stiffness H of a sandwich, which we do next.

2.02.4.4 Shear Stiffness Associated with Second-order Strain

Let us imagine a homogeneous pure shear deformation of an element Δx of the sandwich column:

$$u_1 = u_{1,1} = u_{1,3} = e_{11} = 0,$$
$$u_{3,1} = \gamma, \quad e_{13} = e_{31} = \gamma/2 \qquad (49)$$

With these expressions, the second-order small incremental potential energy of the element, corresponding to (first-order) small strains, is

obtained as

$$\delta^2 W = \Delta x \int_A \left[-\frac{P}{2bt}\left(\frac{1}{2}u_{k,1}u_{k,1} - \alpha e_{k1}e_{k1}\right) \right. $$
$$\left. + \frac{1}{2}G_m\gamma^2 \right] \mathrm{d}A \qquad (50)$$

Upon rearrangements, the incremental potential energy (per height of column, $\Delta x = 1$) is

$$\delta^2 W = bh\Delta x \left(G^{(m)} - \frac{2+m}{4}\frac{P}{bh}\right)\frac{\gamma^2}{2} \qquad (51)$$

In particular, for $m = 2$ (Engesser type) and $m = -2$ (Haringx type),

$$\delta^2 W = \begin{cases} bh\,\Delta x\,\left[G^{(2)} - (P/bh)\right]\gamma^2/2 \\ \quad \text{(Engesser type } G) \\ bh\,\Delta x\; G^{(-2)}\gamma^2/2 \\ \quad \text{(Haringx type } G) \end{cases} \qquad (52)$$

Since the foam core in an axially loaded sandwich column carries no appreciable axial stresses, we should use that definition of $G^{(m)}$ for which the shear stiffness of the core requires no correction for the effect of the axial force P carried by the skins. As we see, that is the latter, Haringx-type, expression (for $m = -2$). In that case, the shear modulus $G^{(-2)}$ is the same as that obtained in a pure shear test without normal stress, e.g., in the torsion test of a thin-wall tube made of the rigid foam.

The solutions for $m \neq -2$, including the Engesser-type formula, are, of course, equivalent. But if they are used, the shear modulus of the core must be corrected for the effect of the axial forces $F = P/2$ carried by the skins. It would be wrong to use in them the G value measured in a pure shear test of the foam, in which no normal force acts on the shear plane.

Intuitive understanding can be gained from Figure 13 (right), which shows two kinds of shear deformation of an element (of height $\Delta x = 1$) of a sandwich column. In the first kind (Figure 13, top right), corresponding to the deformation described by Equation (49), the shearing of the element is accompanied by second-order axial extension of the skins, equal to

$$\delta^2 u = 1 - \cos\gamma \approx \gamma^2/2 \qquad (53)$$

(per unit height). If the initial forces F were negligible, this second-order small extension would make no difference but since they are not, one must take into account the work of the initial forces of F on this extension, which is

$$\delta^2 W = (2F\gamma^2/2)bh \quad \text{or} \quad -bhS^0(-\gamma^2/2) \qquad (54)$$

(per unit height, $\Delta x = 1$). This work must be added to the work of the shear stresses,

$$\delta^2 W = (G\gamma^2/2)bh \qquad (55)$$

in order to obtain the complete second-order work expression. In the second kind of shear deformation (Figure 13, bottom right), the initial forces F do no work. So, the incremental second-order work expressions for these two kinds of shear deformation, respectively, are

$$\delta^2 W = \begin{cases} bh\left(G^{(2)} + S^0\right)\gamma^2/2 & \text{(case a)} \\ G^{(-2)}\gamma^2/2 & \text{(case b)} \end{cases} \qquad (56)$$

These two cases (Figure 13 right) give the same incremental second-order work if $G^{(2)} = G^{(-2)} - S^0$ or $G^{(2)} = G^{(-2)} + 2F/bh$. We see that these relations coincide with (37).

From the foregoing comparisons and the discussion of Figure 13 (right), it is now obvious that a constant shear modulus G, equal to the shear modulus obtained in a shear test of the foam (e.g., a torsional test of a hollow tube), can be used only in the Haringx-type formula ($m = -2$).

Kardomateas *et al.* (2002) and others studied the differences between the Engesser-type and Haringx-type formulas experimentally and by FE analysis. They concluded that the Haringx-type formula gives better predictions. Since they tacitly adopted a constant value of incremental modulus G, this is indeed the conclusion that they should have obtained. The present theoretical analysis explains why.

When can the differences between the column solutions for different m, and particularly between the formulas of Engesser and Haringx, be ignored? When $P \ll H^{(m)} = G^{(m)}bh$.

2.02.4.5 Differential Equations of Equilibrium Associated with Different Finite-strain Measures

The Engesser and Haringx formulas can also be derived from the differential equations of equilibrium. This is discussed for a homogeneous column weak is shear on p. 738 in Bažant and Cedolin (1991), and we will now indicate it for a sandwich. Figure 13 (right) shows two kinds of cross sections of a sandwich column in a deflected position: (a) the cross section that is normal to the deflected column axis, on which the shear force due to axial load is

$$Q = Pw' \qquad (57)$$

and (b) the cross section that was normal to the column axis in the initial undeflected state, on

which the shear force due to axial load is

$$\bar{Q} = P\psi \tag{58}$$

From equilibrium, for a simply supported (hinged) column, the bending moment is $M = -Pw$ in both cases. The force-deformation relations are

$$M = Ebth^2\psi'/2, \tag{59}$$

and

$$Q \text{ or } \bar{Q} = Gbh\gamma \text{ or } Gbh(w' - \psi) \tag{60}$$

in case a or b, respectively. Eliminating M, γ, ψ and Q or $\bar{Q}$ from the foregoing relations, we get a differential equation of the form $w'' + k^2 w = 0$, i.e., the same as Equation (45), where

$$k^2 = \frac{GbhP}{E(bth^2/2)(Gbh - P)} \tag{61}$$

or

$$k^2 = \frac{P^2 + GbhP}{E(bth^2/2)Gbh} \tag{62}$$

respectively. Setting $k = \pi/l$ and solving for P, we find the former equation to lead to Engesser's formula (35) and the latter to Haringx's formula (36). As we see, Engesser's formula ($m = 2$) is obtained when the shear deformation γ is assumed to be caused by the shear force acting on the cross-section that is normal to the deflected axis of column, and Haringx's formula ($m = -2$) when caused by the shear force acting on the rotated cross section that was normal to the beam axis in the initial state.

The foregoing equilibrium derivation, however, does not show that the values of shear stiffness in both formulas must be different.
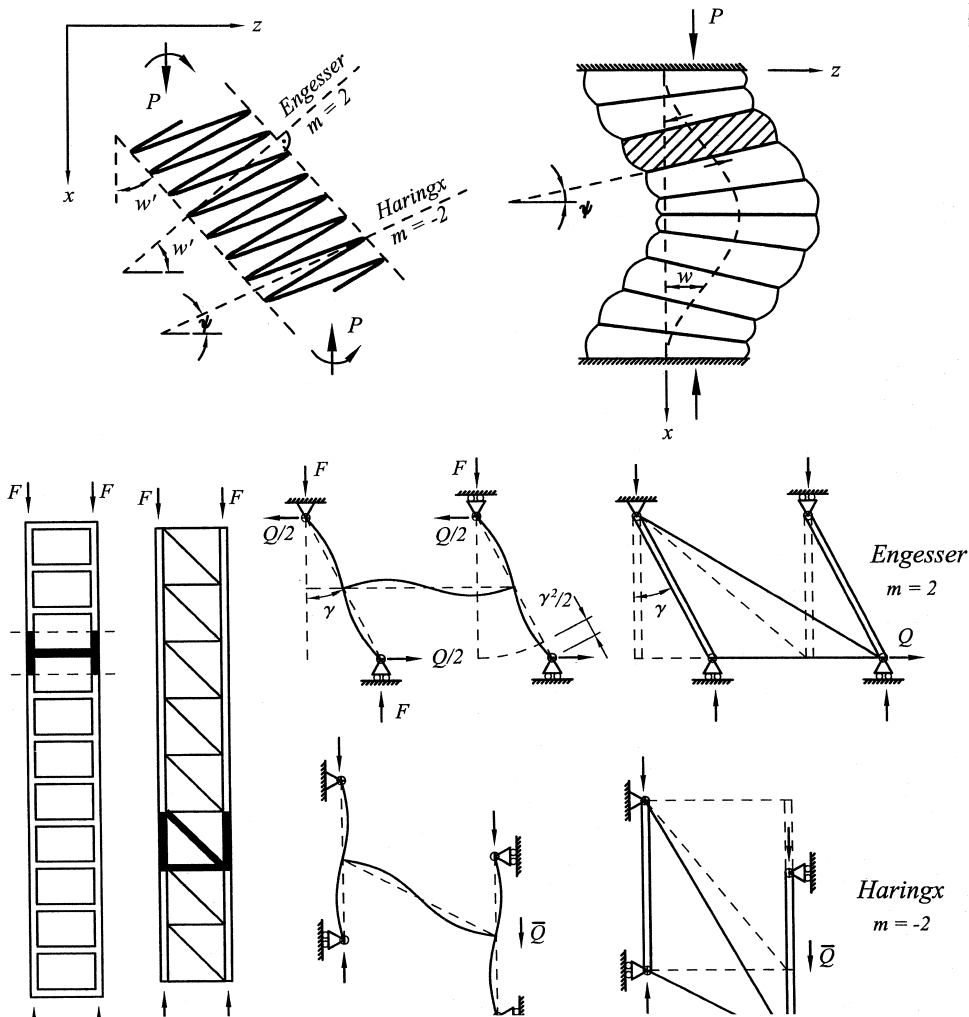
Figure 14 Top left: deformation of a helical spring. Top right: deformation of a layered elastomeric bearing. Bottom left: built-up columns (battened, and pin-jointed lattice). Bottom right: deformations of cells of built-up columns showing second-order axial strain due to shear (top middle and right).

Especially, it does not show that the shear stiffness in the direction of the rotated cross section can be kept constant, while the shear stiffness in the direction of normal to the deflected axis must be considered to depend on the axial force. This has been a perennial source of confusion. To dispel it, the work of the shear forces must be considered, and so, an energy approach is appropriate.

2.02.4.6 Ramifications

The present analysis can be easily adapted to composites with stiff axial fibers and a matrix very soft in shear, as well as to built-up (battened or lattice) columns, helical springs, and layered elastomeric bearings (Figure 14). The conclusions are identical (Bažant, 2002a).

For general structures, Equation (34) is only a necessary condition for making the differences among the finite-strain measures $\varepsilon^{(m)}$ for different m irrelevant. A condition that is sufficient is

$$\max_{(\boldsymbol{x})}||S_{ij}(\boldsymbol{x})|| \ll \min_{(\boldsymbol{x})}||C_{ijkm}^{(m)}(\boldsymbol{x})|| \qquad (63)$$

2.02.5 CLOSING REMARKS

2.02.5.1 Implications for Large-strain FE Analysis

The present conclusions about sandwich buckling have profound implications for large-strain FE analysis in general. The use of the standard updated Lagrangian formulation, in which the constitutive law is defined in terms of the strain rate and the Jaumann (co-rotational) rate of Kirchhoff stress, could not give the correct result for a linearly elastic sandwich column, in which the stress at each point is negligible compared to the elastic moduli at that point. Since the Jaumann rate corresponds to $m = 0$, the result would have to lie in the middle between Haringx's formula ($m = -2$) and Engesser's formula ($m = 2$). The objective stress rate energetically associated with $m = -2$ is the Lie derivative of Kirchhoff stress (Bažant and Cedolin, 1991, section 11.4). Therefore, only this rate can yield the correct FE result.

2.02.5.2 Looking Back and Forward

Historically, a neglect of the shear deformations in built-up columns (which was in conformity to the building code of the time) had one particularly tragic consequence. As shown by Prandtl (1907) and others, disregard of Engesser's (1889) formula by the design code of the time was the main culprit in the collapse in 1907 of the record-span Quebec bridge over St. Lawrence, with a great loss of life.

While there are many examples of theories that have become complete or almost complete, the theory of stability of structures, at the dawn of the third millenium, has not yet reached that point. As far as elastic stability is concerned, its understanding is now very good, although even here a rapid progress has been happening in certain particular directions, for instance those of chaos or general catastrophes. Almost the same could be said of stability of anelastic structures exhibiting plasticity, viscoelasticity, and viscoplasticity.

However, as far as stability of structures disintegrating because of damage and fracture is concerned, this is a challenge for the future. Major advances are still to be expected.

ACKNOWLEDGMENTS

2.02.6 REFERENCES

B. O. Almroth, A. M. C. Holmes and D. O. Brush, 1964, An experimental study of the bulging of cylinders under axial compression. *Exp. Mech.*, **4**, 263.

S. B. Batdorf and B. Budiansky, 1949, "A mathematical theory of plasticity based on the concept of slip," Technical Note No. 1871, Nat. Advisory Committee for Aeronautics, Washington D.C.

Z. P. Bažant, 1971a, Correlation study of formulations of incremental deformations and stability of continuous bodies. *J. Appl. Mech.*, **38**, 919–928.

Z. P. Bažant, 1971b, Micropolar medium as a model for buckling of grid frameworks. In: "Developments in Mechanics," Proceedings of the 12th Midwestern Mechanics conference, U. of Notre Dame, vol. 6, 587–593.

Z. P. Bažant, 1976, Instability, ductility, and size effect in strain-softening concrete. *J. Eng. Mech. Div., Am. Soc. Civil Eng.*, **102**, 331–344 (discussion 103, 357–358, 775–777, 104, 501–502).

Z. P. Bažant, 1980, Work inequalities for plastic-fracturing materials. *Int. J. Solids Struct.*, **16**, 870–901.

Z. P. Bažant, 1982, Crack band model for fracture of geomaterials. In: "Proceedings of the 4th International Conference on Numerical Methods in Geomechanics," ed. Z. Eisenstein, University of Alberta, Edmonton, vol. 3, 1137–1152.

Z. P. Bažant, 1984, Microplane model for strain controlled inelastic behavior. In: "Mechanics of Engineering

Materials," eds. C. S. Desai and R. H. Gallagher, Wiley, London, Chap. 3, 45–59.

Z. P. Bažant, 1986, Mechanics of distributed cracking. *Appl. Mech. Rev.*, **39**, 675–705.

Z. P. Bažant, 1994, Nonlocal damage theory based on micromechanics of crack interactions. *J. Eng. Mech., ASCE*, **120**, 593–617 (addendum and errata 120, 1401–02)

Z. P. Bažant, 1997, Scaling of quasibrittle fracture: Asymptotic analysis. *Int. J. Fract.*, **83**, 19–40.

Z. P. Bažant, 1999, Size effect on structural strength: a review. *Arch. Appl. Mech.*, **69**, 703–725 (75th Anniversary Issue). Reprinted in "Handbook of Materials Behavior," ed. J. Lemaitre, Academic Press, San Diego, 2001, vol. 1, pp. 30–68.

Z. P. Bažant, 2000, Stability of elastic, anelastic and disintegrating structures: a conspectus of main results. *Appl. Math. Mech., ZAMM*, **80**, 709–732. (Ludwig Prandtl's 125th anniversary issue).

Z. P. Bažant, 2001, Scaling of failure of beams, frames and plates with softening hinges. *Meccanica*, **36**, 67–77, (special issue honoring G. Maier).

Z. P. Bažant, 2002a, "Scaling of Structural Strength," Hermes-Penton, London.

Z. P. Bažant, 2002b, Shear buckling of sandwich, fiber-composite and lattice columns, bearings and helical springs: paradox resolved. *J. Appl. Mech.*, ASME, **69**, in press.

Z. P. Bažant and L. Cedolin, 1991, "Stability of Structures: Elastic, Inelastic, Fracture and Damage Theories." Oxford University Press, New York (2nd updated edn., Dover Publications 2003).

Z. P. Bažant and E.-P. Chen, 1997, Scaling of structural failure. *Appl. Mech. Rev.*, **50**, 593–627.

Z. P. Bažant, W.-H. Gu and K. T. Faber, 1995, Softening reversal and other effects of a change in loading rate on fracture of concrete. *ACI Mat. J.*, **92**, 3–9.

Z. P. Bažant and M. Jirásek, 1996, Softening-induced dynamic localization instability: seismic damage in frames. *ASCE J. Eng. Mech.*, **122**, 1149–1158.

Z. P. Bažant and M. Jirásek, 2002, Nonlocal integral formulations of plasticity and damage: survey of progress. *J. Eng. Mech.,* ASCE, **128**, 1119–1149 (ASCE 150th Anniversary Article).

Z. P. Bažant and J.-J. H. Kim, 1998, "Size effect in penetration of sea ice plate with part-through cracks. I. Theory. II. Results." *J. Eng. Mech.,* ASCE, **124**, 1310–1315, 1316–1324.

Z. P. Bažant, J.-J. H. Kim, I. M. Daniel, E. Becq-Giraudon and Goangseup Zi, 1999, Size effect on compression strength of fiber composites failing by kink band propagation. *Int. J. Fract.,* **95**, 103–141 (special issue on Fracture Scaling, eds. Z. P. Bažant and Y. D. S. Rajapakse).

Z. P. Bažant and Y.-N. Li, 1997, "Cohesive crack with rate-dependent opening and viscoelasticity: I. mathematical model and scaling; II. Numerical algorithm, behavior and size effect." *Int. J. Fract.*, **86**, 247–265, 267–288.

Z. P. Bažant and B.-H. Oh, 1983, Crack band theory for fracture of concrete. *Mat. Struct. RILEM, Paris*, **16**, 155–177.

Z. P. Bažant and B.-H. Oh, 1986, Efficient numerical integration on the surface of a sphere. *Zeitschrift für angewandte Mathematik und Mechanik, ZAMM*, **66**, 37–49.

Z. P. Bažant and J. Planas, 1998, "Fracture and Size Effect in Concrete and other Quasibrittle Materials," CRC Press, Boca Raton, Florida, and London.

Z. P. Bažant and Y. Xiang, 1997a, Inelastic buckling of concrete column in braced frame. *J. Struct. Eng.*, **123**, 634–642.

Z. P. Bažant and Y. Xiang, 1997b, Postcritical imperfection-sensitive buckling and optimal bracing of large regular frames. *J. Struct. Eng.*, **123**, 513–522.

T. Belytschko, J. Fish and B. E. Engelmann, 1988, A finite element method with embedded localization zones. *Comp. Meth. Appl. Math. Eng.*, **70**, 59–89.

C. B. Biezeno and H. Hencky, 1928, On the general theory of elastic stability. In: "Proceedings of the Section of Sciences," Koninklijke Akademie van Wettenschappen te Amsterdam, vol. 31, 1928, pp. 569–92 (Meetings Dec. 1927, Jan. 1928), and vol. 32, 1929, pp. 444–56 (April 1929 Meeting).

M. A. Biot, 1965, "Mechanics of Incremental Deformations," Wiley, New York.

V. Bolotin, 1969, "Statistical Methods in Structural Mechanics," Holden-Day, San Francisco, chap. 4.

M. Brocca and Z. P. Bažant, 2000, Microplane constitutive model and metal plasticity. *Appl. Mech. Rev.*, **53**, 265–281.

C. A. Bronkhorst, S. R. Kalindindi and L. Anand, 1992, Polycrystalline plasticity and the evolution crystallographic texture in FCC metals. *Phil. Trans. Roy. Soc. A*, **341**, 443–477.

B. Budiansky, 1974, Theory of buckling and post-buckling of elastic structures, *Advances of Applied Mechanics* 14, ed. C. S. Yih, Academic Press, New York, pp. 1–65.

B. Budiansky, 1983, Micromechanics. *Comp. Struct.*, **16**, 3–12.

B. Budiansky and J. W. Hutchinson, 1964, Dynamic Buckling of Imperfection-Sensitive Structures. In: "Proceedings of the 12th International Congress on Applied Mechanics, Munich," pp. 636–651.

B. Budiansky and J. W. Hutchinson, 1972, Buckling of circular cylindrical shells under axial compression. In: "Contributions to the Theory of Aircraft Structures," Delft University Press, The Netherlands, pp. 239–260.

G. C. Butler and D. L. McDowell, 1998, Polycrystal constraint and grain sub-division. *Int. J. Plast.*, **14**, 703–717.

F. C. Caner, Z. P. Bažant and J. Červenka, 2002, Vertex effect in strain-softening concrete at rotating principal axes. *J. Eng. Mech.,* ASCE, **128**, 24–33.

I. Carol and Z. P. Bažant, 1997, Damage and plasticity in microplane theory. *Int. J. Solids Struct.*, **34**, 29 3807–3835.

B. A. Cotter and R. S. Rivlin, 1955, Tensors associated with time-dependent stress. *Quart. Appl. Math.*, **13**, 177–182.

J. Červenka and V. Červenka, 1998, Fracture-plastic material model for concrete. In: "Fracture Mechanics of Concrete Structures, Proceedings of the 5th International Conference FraMCoS-5, Gifu, Japan," eds. H. Mihashi and K. Rokugo, Aedification Publ., Freiburg, Germany, pp. 1107–1116.

F. C. Caner and Z. P. Bažant, 2000, Microplane model M4 for concrete: II. Algorithm and Calibration. *J. Eng. Mech.,* ASCE, **126**, 954–961.

F. C. Caner, Z. P. Bažant and J. Červenka, 2000, "Vertex effect in strain-softening concrete at rotating principal axes," Structural Mechanics Report, Northwestern University; also *J. Eng. Mech.,* ASCE, **128**, 24–33.

E. Chwalla, 1928, "Die Stabilität zentrisch und exzentrisch gedrückter Stäbe aus Baustahl," Sitzungsberichte der Akademie der Wissenschaften in Wien, Part IIa, p. 469.

R. de Borst, 1987, Computation of post-bifurcation and post-failure behavior of strain-softening solids. *Comp. Struct.*, **25**, 211–224.

R. de Borst, 1988, Bifurcations in finite element models with a nonassociated flow law. *Int. J. Num. Anal. Meth. Geomech.*, **12**, 99–116.

R. de Borst, 1989, Numerical methods for bifurcation analysis in geomechanics. *Ingenieur-Archiv*, **59**, 160–174.

L. H. Donnell, 1934, A new theory for the buckling of thin cylinders under axial compression and bending. *Trans. ASME*, **56**, 795–806.

T. C. Doyle and J. L. Ericksen, 1956, Nonlinear elasticity. *Advances Appl. Mech.*, **4**, 53–115.

D. C. Drucker, 1951, A more fundamental approach to plastic stress–strain relations. In: "Proceedings of the 1st US National Congress of Applied Mechanics," (ASME), pp. 487–491.

F. Engesser, 1889, Die Knickfestigkeit gerader Stäbe. *Z. Architekten und Ing. Vereins zu Hannover*, **35**, 455.

F. Engesser, 1895, Über Knickfragen. *Schweizerische Bauzeitung*, **26**, 24–26.

F. Engesser, 1898, *Z. ver. deut. Ingr.* **42**, 927; see also 1899, Über die Knickfestigkeit gerader Stäbe. *Zeitschrift für Architecktur und Ingenieurwesen*, **35**.

A. C. Eringen, 1965, Theory of micropolar continuum. In: "Proceedings of the 9th Midwestern Mechanics Conference," University of Wisconsin, Madison, pp. 23–40.

L. Euler, 1744, *Methodus inveniendi lineas curvas maximi minimive porprietate gaudentes.* In: "Appendix, De Curvis Elasticis," Marcum Michaelem Bosquet, Lausanne.

N. A. Fleck, 1997, Compressive failure of fiber composites. *Adv. Appl. Mech.*, **33**, 43–117.

A. Föppl, 1907, "Vorlesungen über technische Mechanik," Druck und Verlag von B. G. Teubner, Liepzig, vol. 5, p. 132.

A. M. Freudenthal, 1950, "The Inelastic Behavior of Engineering Materials and Structures," Wiley, New York.

G. Gerard and H. Becker, 1957, "Handbook of structural stability. Part I: buckling of flat plates," NACA Technical Note No. 3781.

J. Hadamard, 1903, "Leçons sur la propagation des ondes," Hermann Paris chap. 6.

J. A. Haringx, 1942, On the buckling and lateral rigidity of helical springs. *Proc. Konink. Ned. Akad. Wet.*, **45**, 533 see also Timoshenko and Gere (1961), p. 142.

R. Hill, 1950, "The Mathematical Theory of Plasticity," Oxford University Press, Oxford, UK.

R. Hill, 1958, A general theory of uniqueness and stability in elastic-plastic solids. *J. Mech. Phys. Solids*, **6**, 236–249.

R. Hill, 1962, Uniqueness criteria and extremum principles in self-adjoint problems of continuum mechanics. *J. Mech. Phys. Solids*, **10**, 185–194.

H. H. Hilton, 1952, Creep collapse of viscoelastic columns with initial curvatures. *J. Aero. Sci.*, **19**, 844–846.

N. J. Hoff, 1958, A survey of the theories of creep buckling. In: "Proceedings of the 3rd US National Congress Applied on Mechanics, Providence, RI," pp. 29–49.

E. Hurlbrink, 1908, *Schiffbau*, **9**, 517.

J. W. Hutchinson, 1970, Elastic plastic behavior of polycrystalline metals and composites. *Proc. Roy. Soc. A*, **139**, 247–272.

J. W. Hutchinson, 1974, Plastic buckling. *Adv. Appl. Mech.*, **14**, 67–144.

J. W. Hutchinson and K. W. Neale, 1978, Sheet Necking. II. Time-independent behavior. In: "Mechanics of Sheet Metal Forming," eds. D. K. Koistinen and N.-M. Wang, Plenum, New York.

J. W. Hutchinson and V. Tvergaard, 1980, *Int. J. Mech. Sci.*, **22**, 339.

B. W. James, 1935, "Principal effects of axial load by moment distribution analysis of rigid structures," NACA Technical Note No. 534.

G. Jaumann, 1911a, Geschlossenes System physikalischer und chemischer Differentialgesetze. *Sitzungsberichte Akad. Wiss. Wien IIa*, **120**, 385–530.

M. Jirásek, 1998a, Embedded crack models for concrete fracture. In: Proceedings of the Conference on Computational Modeling of Concrete Structures (EURO-C), Badgastein, Austria, ed. R. de Borst *et al.* Balkema, Rotterdam, 291–300.

M. Jirásek, 1998, Nonlocal models for damage and fracture: comparison of approaches. *Int. J. Solids Struct.*, **35**, 4133–4145.

M. Jirásek and Z. P. Bažant, 2002, "Inelastic Analysis of Structures." Wiley, London and New York 735 + xviii pp.).

G. A. Kardomateas, G. J. Simitses, L. Shen and R. Li, 2002, Buckling of sandwich wide columns. *Int. J. Nonlinear Mech.*, **37**, 1239–1247 (Special issue on "Nonlinear Stability of Structures").

G. R. Kirchhoff, 1859, Über das Gleichgewicht und die Bewegung eines unendlich dünnen elastischen Stabes. *J. Math. (Crelle)*, **56**, 285–313.

W. T. Koiter, 1945, Over de stabiliteit van het elastische evenwicht. Dissertation, Delft, Holland. Translation: On the Stability of Elastic Equilibrium. NASA TT-F-10833, 1967, and AFFDL-TR-70-25, 1970.

W. T. Koiter, 1953, Stress–strain relations, uniqueness and variational theorems for elastic–plastic materials with a singular yield surface. *Q. Appl. Math.*, **11**, 350–354.

L. Kollár and E. Dulácska, 1984, "Buckling of Shells for Engineers," Wiley, Chichester, UK.

J. L. Lagrange, 1788, "Mécanique Analytique," Courier, Paris.

Y. Leroy and M. Ortiz, 1989, Finite element analysis of strain localization in frictional materials. *Int. J. Numer. Anal. Meth. Geomech.*, **13**, 53–74.

Y. N. Li, A. N. Hong and Z. P. Bažant, 1995, Initiation of parallel cracks from surface of elastic half-plane. *Int. J. Fract.*, **69**, 357–369.

A. M. Liapunov, 1893, Issledovanie odnogo iz ossobenykh sluchaev zadachi ob ustoichivosti dvizhenia. *Matem. Sbornik.*, **17**, 253–333.

R. K. Livesley and D. B. Chandler, 1956, "Stability functions for structural frameworks," Manchester University Press, Manchester.

R. Lorenz, 1908, Achsensymmetrische Verzerrungen in dünnwandingen Hohlzylindern. *Zeitschrift des Vereines Deutscher Ingenieure*, **52**, 1706–1713.

L. Kollár and E. Dulácska, 1984, "Buckling of Shells for Engineers," Wiley, Chichester, England.

G. Maier, A. Zavelani and J. C. Dotreppe, 1973, Equilibrium branching due to flexural softening. *J. Eng. Mech.*, **99**, 897–901.

J. Mandel, 1964, "Conditions de stabilité et postulat de Drucker." In: "Rheology and Soil Mechanics, Proceedings of the IUTAM Symposium Grenoble," eds. J. Kravtchenko and P. M. Sireys, Springer, Berlin, 58–68.

A. G. M. Michell, 1899, *Phil. Mag.*, **48**, 298.

F. C. Moon, 1986, "Chaotic Vibrations," Wiley, New York.

A. Needleman, 1982, A numerical study of necking in circular cylindrical bars. *J. Mech. Phys. Solids*, **20**, 111–120.

H. Neuber, 1965, Theorie der elastischen Stabilität bei nichtlinearer Vorverformung. *Acta Mech.*, **3**, 285.

Q. S. Nguyen, 1987, Bifurcation and postbifurcation analysis in plasticity and brittle fracture. *J. Mech. Phys. Solids*, **35**, 303–324.

R. W. Ogden, 1984, "Nonlinear Elastic Deformations," Ellis Horwood and Wiley, Chichester, UK.

J. G. Oldroyd, 1950, On the formulation of rheological equations of state. *Proc. Roy. Soc. A*, **200**, 523–541.

M. Ortiz, Y. Leroy and A. Needleman, 1987, A finite element method for localized failure analysis. *Comp. Meth. Appl. Mech, i Eng.*, **61**, 189–214.

W. R. Osgood, 1951, "The effect of residual stress on column strength." In: "Proceedings of the 1st US National Congress of Applied Mechanics," p. 415.

R. H. J. Peerlings, R. de Borst, W. Brekelmans and J. Vre, 1996b, Gradient enhanced damage for quasibrittle materials. *Int. J. Num. Meth. Eng.*, **39**, 3391–3403.

H. Petryk, 1985, On stability and symmetry condition in time-dependent plasticity. *Arch. Mech. Stos. (Warsaw)*, **37**, 503–520.

F. J. Plantema, 1966, "Sandwich Construction: The Bending and Buckling of Sandwich Beams, Plates and Shells," Wiley, New York.

L. Prandtl, 1899, Kipperscheinungen. Dissertation, Technical University, München.

L. Prandtl, 1907, *Z. Verein Deutscher Ing.*

L. Prandtl, 1924, Spannungsverteilung in plastischen Körpern. In: "Proceedings of the 1st International Congress of Applied Mechanics," Delft, Technische Boekhandel en Druckerij, J. Waltmann, Jr., 43–54.

J. W. S. Rayleigh, 1894, "The Theory of Sound," Macmillan, New York; Dover Publications, New York, 1945, vol. 1.

J. R. Rice, 1971, Inealastic constitutive relations for solids: an internal variable theory and its application to metal plasticity. *J. Mech. Phys. Solids*, **19**, 433–455.

J. R. Rice, 1975, On the stability of dilatant hardening in saturated rock masses. *J. Geophys. Res.*, **80**, 1531–1536.

J. R. Rice, 1976, "The localization of plastic deformation," In: Proceedings of the Congress of Theoretical and Applied Mechanics, Delft, The Netherlands, vol. 1, pp. 207–220.

J. R. Rice, 1993, Mechanics of solids. "Encyclopedia Britanica" 15th edn., vol. 23, 737–747, 773.

J. R. Rice and A. L. Ruina, 1982, Stability of steady frictional slipping. *J. Appl. Mech.*, **50**, 343–349.

J. Roorda, 1971, An experience in equilibrium and stability, Techn. Note No. 3, Solid Mech. Div., University of Waterloo, Canada.

B. W. Rosen, 1965, Mechanics of composite strengthening. In: "Fiber Composite Materials," American Society for Metals Seminar, Chap. 3, American Society for Metals, Metals Park, OH, pp. 37–75.

J. W. Rudnicki and J. R. Rice, 1975, Conditions for the localization of deformation in pressure-sensitive dilatant materials. *J. Mech. Phys. Solids*, **23**, 371–394.

F. R. Shanley, 1947, Inelastic column theory. *J. Aero. Sci.*, **14**, 261–268.

E. Simiu and R. H. Scanlan, 1986, "Wind Effects on Structures: An Introduction to Wind Engineering," 2nd edn., Wiley, New York.

J. Singer, J. Arbocz and T. Weller, 1998, "Buckling Experiments," Wiley, New York.

R. V. Southwell, 1914, On the general theory of elastic stability. *Phil. Trans. Roy. Soc. London, A*, **213**, 187–244.

L. Strömberg and M. Ristinmaa, 1996, FE-formulation of a nonlocal plasticity theory. *Comp. Meth. Appl. Mech. Eng.*, **136**, 127–144.

G. I. Taylor, 1938, Plastic strain in metals. *J. Inst. Metals*, **62**, 307–324.

R. C. Tennyson, 1969, Buckling modes of circular cylindrical shells under axial compression. *AIAA J.*, **7**, 1481.

R. C. Tennyson and K. C. Chan, 1990, Buckling of imperfect sandwich cylinders under axial compression. *Int. J. Solids Struct.*, **26**, 1017–1036.

R. Thom, 1975, "Structural Stability and Morphogenesis," transl. D. H. Fowler, Benjamin, Reading.

J. M. T. Thompson, 1982, "Instabilities and Catastrophes in Science and Engineering," Wiley, Chichester, New York.

J. M. T. Thompson, 1989, Chaotic dynamic and the newtonian legacy. *Appl. Mech. Rev.*, **42**, 15–25.

J. M. T. Thompson and H. B. Stewart, 1986, "Nonlinear Dynamics and Chaos," Wiley, Chichester, New York.

S. P. Timoshenko, 1910, Einige Stabilitätsprobleme der Elastizitätstheorie. *Zeitschrift für Angew. Math. Phys.*, **58**, 337–385.

S. P. Timoshenko, 1921, On the correction for shear in the differential equation of transverse vibrations of prismatic bars. *Phil. Mag. 6*, **21**, 747.

S. P. Timoshenko and J. M. Gere, 1961, "Theory of Elastic Stability," McGraw-Hill, New York.

C. Truesdell, 1955, The simplest rate theory of pure elasticity. *Comm. Pure Appl. Math.*, **8**, 123–132.

V. Tvergaard, 1982, On localization in ductile materials containing spherical voids. *Int. J. Fract.*, **18**, 237–252.

J. G. M. van Mier, 1986, Multiaxial strain-softening of concrete. *Mat. Struct.*, **19**, 179–200.

T. von Kármán, 1910, Untersuchungen über Knickfestigkeit. *Mitteilungen über Forschungsarbeiten auf dem Gebiete des Ingenieurwesens*, **81**.

T. von Kármán, E. E. Sechler and L. H. Donnell, 1932, The strength of thin plates in compression. *Trans. ASME*, **54**, 53–58.

T. von Kármán and H. S. Tsien, 1941, The buckling of thin cylindrical shells under axial compression. *J. Aero. Sci.*, **8**, 303–312.

R. von Mises and J. Ratzersdorfer, 1926, Die Knicksicherheit von Rahmentragwerken. "*Zeitschrift für Angew. Math. und Mech.*", vol. 6, p. 181.

C. H. Yang, L. S. Beedle and B. G. Johnston, 1952, Residual stress and the yield strength of steel beams. *Weld. J. (suppl.)*, **31**, 205–229.

T. Young, 1807, "A Course of Lectures on Natural Philosophy and the Mechanical Arts." London, vol. 1, p. 144.